



UNIVERSITY OF LEEDS

This is a repository copy of *Distribution of contourite drifts on convergent margins: Examples from the Hikurangi subduction margin of New Zealand*.

White Rose Research Online URL for this paper:  
<https://eprints.whiterose.ac.uk/162862/>

Version: Accepted Version

---

**Article:**

Bailey, WS, McArthur, AD [orcid.org/0000-0002-7245-9465](https://orcid.org/0000-0002-7245-9465) and McCaffrey, WD [orcid.org/0000-0003-2895-3973](https://orcid.org/0000-0003-2895-3973) (2021) Distribution of contourite drifts on convergent margins: Examples from the Hikurangi subduction margin of New Zealand. *Sedimentology*, 68 (1). pp. 294-323. ISSN 0037-0746

<https://doi.org/10.1111/sed.12779>

---

© 2020 The Authors. *Sedimentology* © 2020 International Association of Sedimentologists. This is the peer reviewed version of the following article: Bailey, W.S., McArthur, A.D. and McCaffrey, W.D. (2020), Distribution of contourite drifts on convergent margins: Examples from the Hikurangi subduction margin of New Zealand. *Sedimentology*. doi:10.1111/sed.12779, which has been published in final form at <https://doi.org/10.1111/sed.12779>. This article may be used for non-commercial purposes in accordance with Wiley Terms and Conditions for Use of Self-Archived Versions. Uploaded in accordance with the publisher's self-archiving policy.

**Reuse**

Items deposited in White Rose Research Online are protected by copyright, with all rights reserved unless indicated otherwise. They may be downloaded and/or printed for private study, or other acts as permitted by national copyright laws. The publisher or other rights holders may allow further reproduction and re-use of the full text version. This is indicated by the licence information on the White Rose Research Online record for the item.

**Takedown**

If you consider content in White Rose Research Online to be in breach of UK law, please notify us by emailing [eprints@whiterose.ac.uk](mailto:eprints@whiterose.ac.uk) including the URL of the record and the reason for the withdrawal request.



[eprints@whiterose.ac.uk](mailto:eprints@whiterose.ac.uk)  
<https://eprints.whiterose.ac.uk/>

## **Distribution of contourite drifts on convergent margins: examples from the Hikurangi subduction margin of NZ**

William S. Bailey, Adam D. McArthur, and William D. McCaffrey

*Turbidites Research Group (TRG), School of Earth and Environment, University of Leeds,  
Leeds, LS2 9JT, UK*

*Email: W.S.Bailey03@gmail.com*

### **ABSTRACT**

Contourite drift systems form a significant component of the marine clastic sedimentary record. Although contourites form in all tectonic settings, few studies have described their development along convergent margins; such characterisation is needed to underpin oceanographic and palaeoenvironmental studies in active settings. This study is the first to document contourite drift development along the Hikurangi subduction margin of New Zealand. Integration of bathymetric, seismic and well data enables five classes of drift to be recognised around the subduction wedge, occurring in three principal associations:

1. an upper slope drift association of giant elongate mounded (c.150 km long, 50 km wide, and up to 1,100 metres thick) and plastered drifts (c. 300 km long, 8 km wide and < 600 m thick), which occurs upon and inboard of a major intrabasinal thrust-cored high, whose long axis parallels the coast; shallow bottom currents disperse sub-parallel to this axis;
2. a spatiotemporally discontinuous association of confined and mounded hybrid drifts (c. 500 m long, < 2 km wide, and up to 500 m thick) that occurs along the mid-to-outer

slope domain of the wedge, recording the interaction of along-slope and downslope currents within trench-slope basins;

3. a trench fill assemblage that implies the passage of abyssal bottom currents across a 40 km reach of the trench-axial Hikurangi Channel-levee, with associated modification of the channel form and of overbank sediment waves.

The fundamental presence of contourites along this margin appears to depend on the orientation and strength of oceanographic bottom currents. However, drift type and evolution vary depending on the slope gradient and the presence of irregular seafloor topography created by tectonic structures. The documented drifts are generally smaller, less continuous, and develop more intermittently than similar styles of drifts documented on passive margins; this mode of occurrence may be characteristic of contourite development on convergent margins.

## **INTRODUCTION**

Contourite drift systems, or contourites, are sedimentary packages that are substantially affected by persistent along-slope bottom currents; they may form along any continental margin where along-slope processes dominate those of gravity currents and pelagic/hemipelagic settling processes (Heezen, et al., 1966; Heezen and Hollister, 1971; Rebesco et al., 1996, 2014; Stow et al., 2002, 2008; Hernández-Molina et al., 2008a, 2008b). Contourite drifts cover large areas of the modern seafloor, with individual drifts being of the order of 10 – 1,000 m high and  $>10^6$  km in area (e.g., Erik drift, [Arthur et al., 1989]; Faro drift [Cremer et al., 1985; Mougnot, 1988]; Campos Basin [Faugères et al., 1993, 1998]), commonly with subsidiary contourite bedforms such as waves, dunes, ripples, and scours visible on the seafloor (Stow and Lovell, 1979). Contourites principally occur where the Coriolis force constrains bottom currents to flow parallel to bathymetric strike, but also occur where current velocities increase over steeper intra-slope ridges and through constricting topographic obstacles (e.g., seamounts, channels,

ridges) (Heezen and Hollister, 1964; Flood, 1994; Faugères et al., 1999; Stow et al., 2008; Rebesco et al., 2014). Contourites are typically interbedded with other deposit types. In siliclastic-starved basins they may rework pelagic sediments (Hollister et al., 1974; Lonsdale, 1981; Reed et al., 1987) and mass transport deposits (Faugères and Gonthier, 1997; Hernández-Molina et al., 2008a; Faugères and Mulder, 2011). When turbidite systems are present, contour currents can modify them to different degrees, ranging from reworking turbidite bed tops to complete erosion and redistribution to form stand-alone contourites (e.g., Locker and Laine, 1992; Howe, 1996; Masse et al., 1998; Mulder et al., 2008; Brackenridge et al., 2013; Sansom, 2018; Fonnesu et al., 2020; Fuhrmann et al., 2020). Contourites constitute high-resolution, semi-continuous sedimentary records of past oceanic circulation and climate change with implications for paleo-oceanography, paleoclimatology, and geohazard studies (Mulder et al., 2002; Toucanne et al., 2007; Knutz, 2008; Laberg et al., 2016; Miramontes et al., 2018). The presence of drifts is also significant for hydrocarbon exploration given their potential to modify reservoir, source rock, and seal properties (Viana et al., 2007; Viana, 2008; Hernández-Molina et al., 2008b; Palermo et al., 2014; Rebesco et al., 2014; Sansom, 2018; Fonnesu et al., 2020).

Compared to studies of passive continental margins and abyssal environments the spatiotemporal distribution of contourites along active margins is relatively poorly documented (e.g., the Falklands Trough [Cunningham et al., 2002]; the Weddell Sea [Hernández-Molina et al., 2006, 2008a]; the Eastern Sunda Arc [Reed et al., 1987] and the Sea of Okhotsk [Wong et al., 2003]). This discrepancy principally reflects the presence of vigorous thermohaline bottom currents and associated contourites within the Atlantic and Mediterranean basins which have received much study (e.g., Heezen et al., 1966; Hollister and Heezen, 1972; Hollister et al., 1974; Johnson and Peters, 1979; McCave et al., 1995; Rebesco et al., 2014); it may also arise due to bottom current processes being commonly overlooked in sedimentary studies of modern and ancient convergent margins, where gravity-driven sedimentation is often assumed to

dominate (McCave and Tucholke, 1986; Reed et al., 1987; Schut and Uenzelmann-Neben, 2005; Van Rooij et al., 2010; Thran et al., 2018). Although drifts have been recognised offshore New Zealand (Barnes, 1992; Carter and McCave, 1994; Fulthorpe et al., 2011), these occur at abyssal depths on the Chatham Rise and Pacific Plate, hundreds of kilometres from the convergent margin boundary.

The principal aim of this study is to address the gap in our understanding of how contourites develop on active vs. passive tectonic margins. To this end, we investigate the development of hitherto undocumented sedimentary drifts that occur at a range of water depths along the active plate boundary of the Hikurangi subduction margin, via:

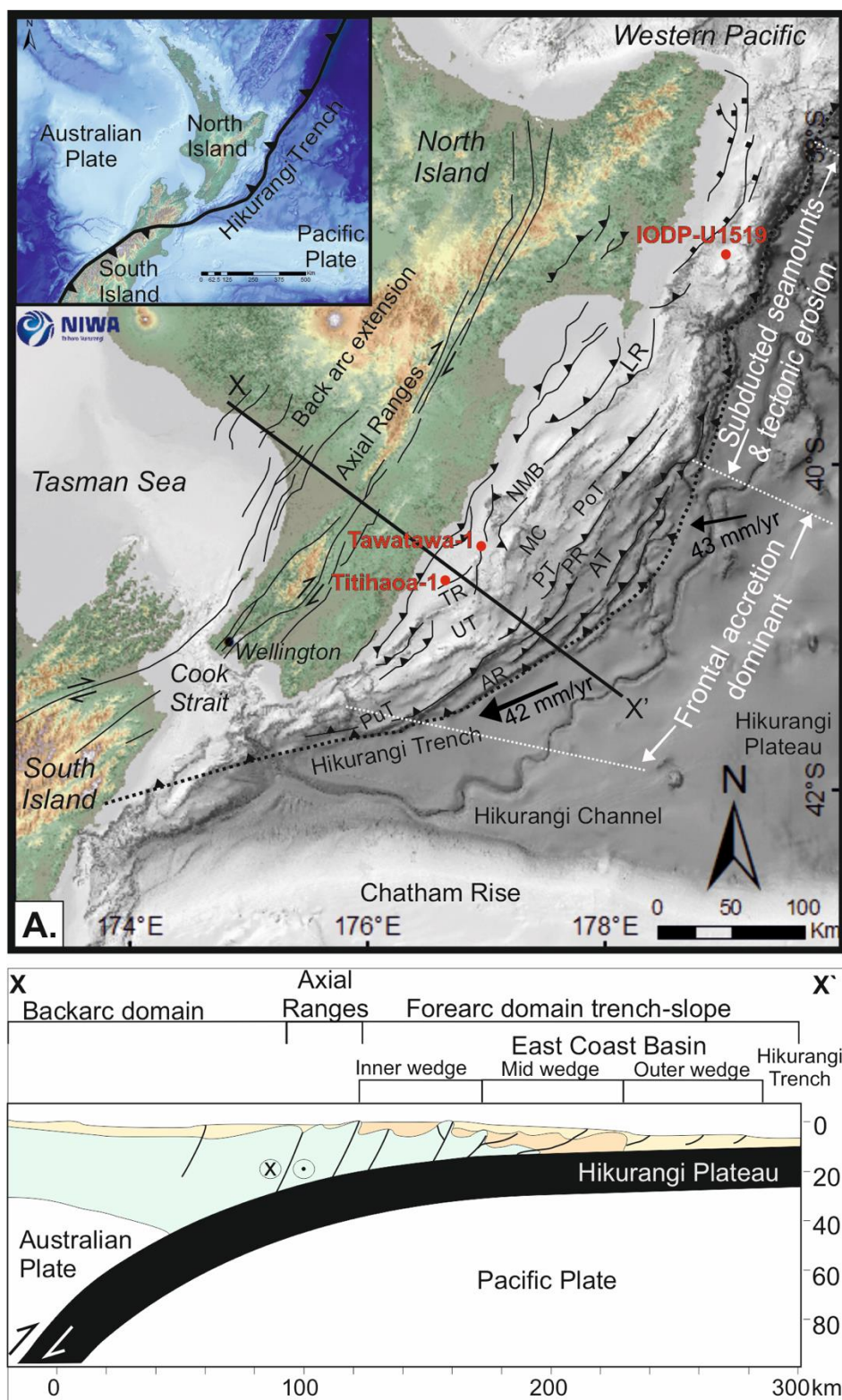
1. Use of high-resolution bathymetry data to characterize sediment wave geometries (*sensu* Wynn and Stow, 2002) on the modern seafloor in order to identify active contourite drift systems.
2. Use of diagnostic seismic features to classify and map key depositional and erosional drift elements in the shallow subsurface, through analysis of over 15,000 line-kilometres of 2D seismic reflection data.
3. Documentation of the interaction between along-slope contouritic systems and downslope gravity current systems in a convergent margin.
4. Constraint of the role of underlying structural features in the generation and subsequent modification of contourite drifts.

Recognition of structural influences on the generation and modification of contourite drifts on the Hikurangi Margin may aid the identification and prediction of contourite distribution on other tectonically active margins affected by bottom currents.

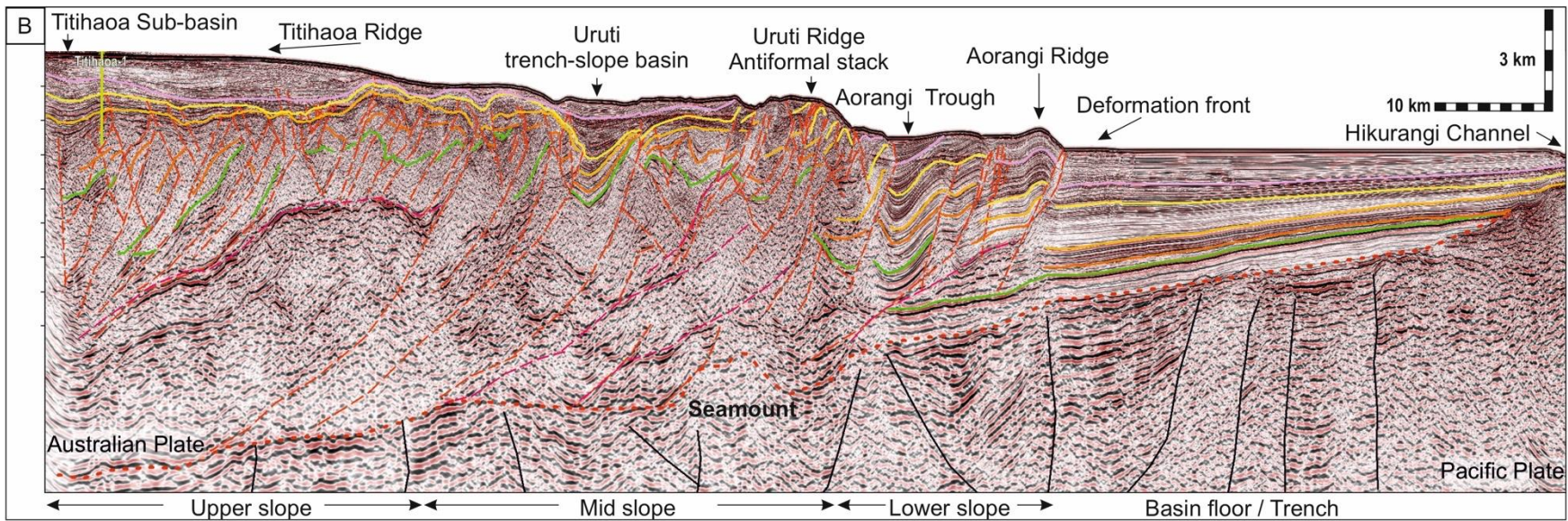
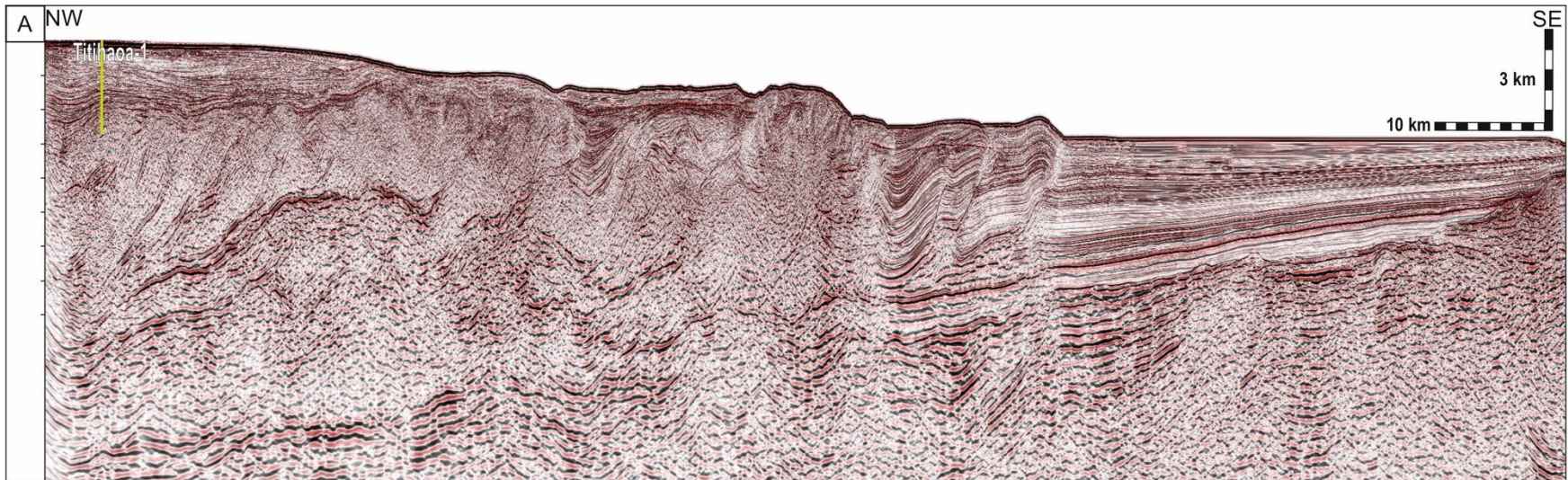
## **GEOLOGICAL AND OCEANOGRAPHIC SETTING**

The study area is located offshore of the North Island of New Zealand, along the actively evolving Hikurangi subduction margin, where the Pacific Plate subducts beneath the Australian Plate (Fig. 1; Lewis and Pettinga, 1993; Nicol et al., 2007; Davy et al., 2008; Bland et al., 2015). Reverse, normal, and strike-slip faults trending ENE-SWS characterize the subduction zone, predominantly forming fold-and-thrust bounded trench-slope basins (Fig. 2; Lewis and Pettinga, 1993; Bailleul, et al., 2013; McArthur et al., 2019). The obliquity of the subduction zone results in strain partitioning across the convergent interface (Nicol et al., 2007; Wallace et al., 2012). The subduction zone accommodates approximately <45% of normal plate-parallel motion; the remaining strain is accommodated in the upper plate through the combination of forward and back thrusts connected to a basal decollement, dextral strike-slip faulting, and vertical axis clockwise rotations (Nicol et al., 2007). Elevated bathymetry and basement depth define the structure of the Hikurangi Margin and partly dictate sedimentation pathways along the continental shelf and slope due to significant structural variation along strike (Wood and Davy, 1994; Barnes et al., 2010; Bland et al., 2015; McArthur et al., 2019).

The development of the modern Hikurangi Trench and subduction wedge began ca. 27 million years ago (Chanier et al., 1999; Barnes et al., 2002; Nicol et al., 2007). A phase of mixed extension and compression occurred during the Middle-to-Late Miocene (Chanier et al., 1999; Nicol et al., 2007); compression continued in the remainder of the wedge thereafter through the Late Miocene to the present, with trench-slope basins filling with deep-water sediments (Lewis and Pettinga, 1993). During the Quaternary, rapid basement uplift occurred, resulting in the development of the present-day fold-and-thrust belt and the modern oceanographic current configuration (Carter et al., 2004; McArthur et al., 2019).



**Fig. 1** (A) Regional setting map and cross section (X-X'). Major intrabasinal features and well locations used in study (red): Akitio Trough (AT); Aorangi Ridge (AR); Lachlan Ridge (LR); Madden Canyon (MC); North Madden Bank (NMB); Paoanui Trough (PoT); Porangahau Ridge (PR); Porangahau Trough (PT); Pukehoho Trough (PuT); Titihaoa Ridge (TR); Uruti Trough (UT). Modified from work by Barnes et al. (2010) and McArthur et al. (2019).





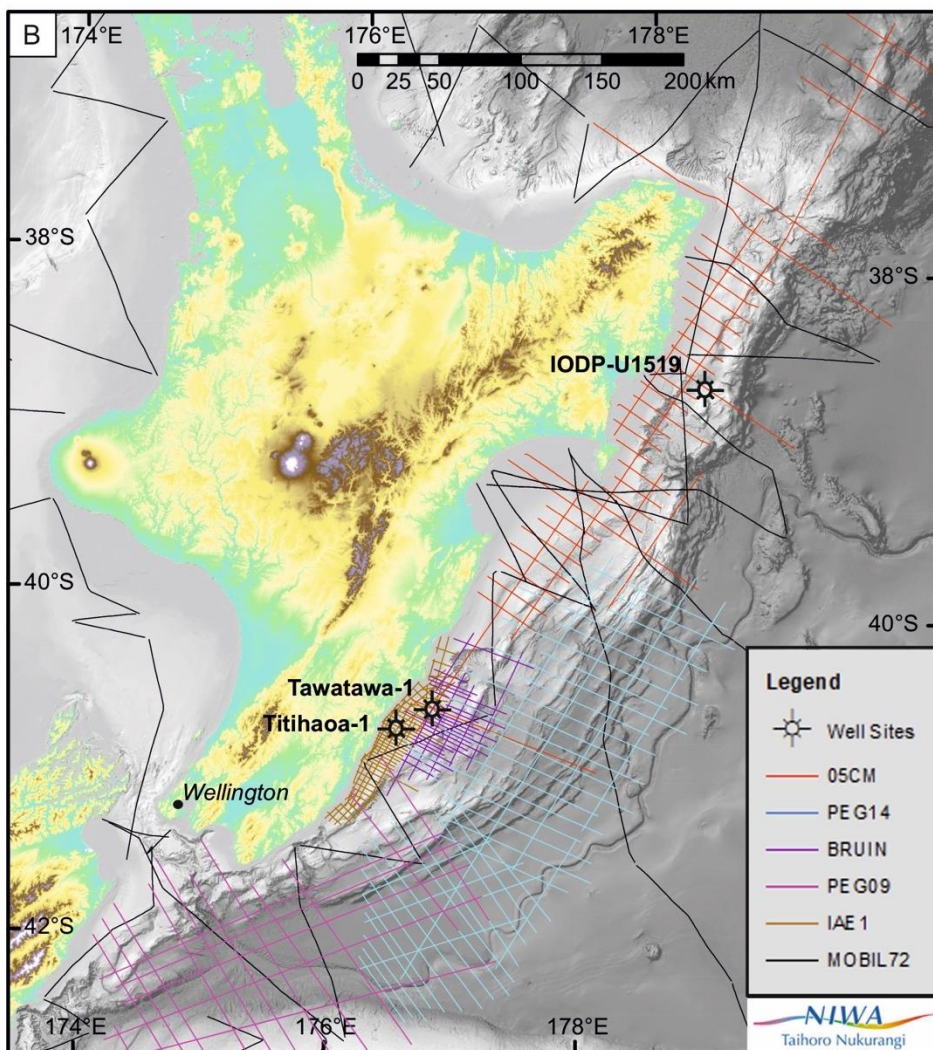
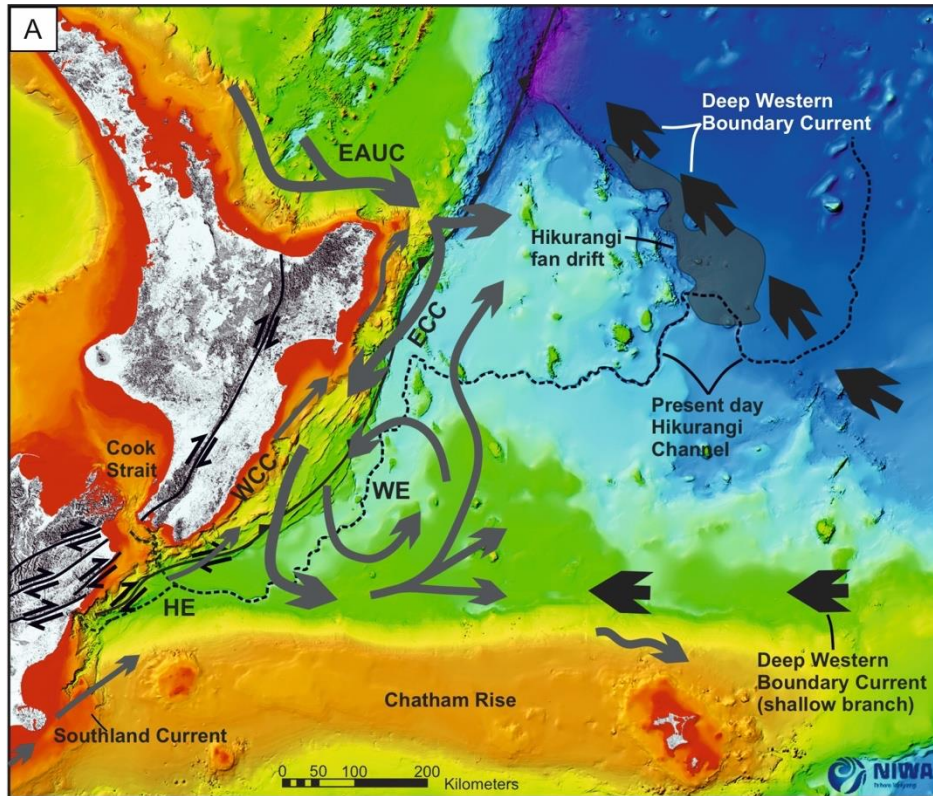
**Fig. 2** (A) Non-interpreted and (B) Interpreted regional NW-SE seismic cross line located in the southern portion of the subduction wedge, illustrating major intrabasinal structures, trench-slope basins and interpreted horizons (modified from McArthur et al., 2019). Data provided by WesternGeco.

The Hikurangi subduction margin forms part of the Eastern New Zealand Oceanic Sedimentary System (Carter et al., 1996). The combination of mechanically weak strata and a humid climate results in the production of large volumes of sediment and its dispersal to the marine environment (Carter et al., 2004), where it may be transported along-shore or ducted offshore via direct or tortuous canyons and channels (e.g., Mountjoy et al., 2009). Some of this marine sediment becomes captured in the trench-slope basins (e.g., Bailleul, et al., 2013). However, much of it is dispersed via deep-ocean conduits (i.e., the Solander, Bounty and Hikurangi channels) to supply abyssal basins (Carter et al., 2004); sediment derived from Zealandia is thereby transported across and along the plate boundary and ultimately fed into the Southwest Pacific Basin (Carter et al., 2004). Eustasy, subsidence, and glaciomarine variations and tectonism strongly influence the along-shore and offshore sediment transport regimes through the Neogene to the present (Fulthorpe et al., 1991, 2011; Carter et al., 1996, 2004; Mountjoy et al., 2018). Significant narrowing of the subduction wedge at the southern and northern region of the margin results in the connection of shelf-attached canyons to the trench-axial Hikurangi Channel, allowing bypass of sediment to the deep-ocean (Carter et al., 2004).

Variations in the ocean circulation system have been recorded from the Oligocene-to-Recent (Carter et al. 2004), reflecting the changing plate tectonic configuration of Zealandia, as well as regional changes in ocean circulation. At the present day, the primary current interacting with the Hikurangi Margin is the Deep Western Boundary Current (DWBC), a major deep-ocean, thermohaline current derived from Antarctica which is active at c. 3,000 m depth (Fig. 3A; Stow et al., 1996; Stickley et al., 2001; Carter et al., 2002, 2004, Chiswell et

al., 2015). Interaction of the DWBC with the East Cape Current (ECC), i.e., the southern extension of the East Auckland Cape Current (EAUC), at depths of c. 2,000 m drives some of the main oceanographic systems along the east coast of New Zealand (Fig. 3A; Warren, 1981; McCave and Carter, 1997; Chiswell and Roemmich, 1998; Chiswell et al., 2015). In addition, a number of smaller currents and eddies, both relatively shallow (less than c. 1,000 m) and deep (c. 1,000 – 2,000 m), are seen to interact with the slope along the subduction margin (Brodie, 1960; Chiswell et al., 2015). Of these subsidiary currents the principal one is the northerly directed, shallow, wind-driven Wairarapa Coastal Current, whose interaction with the ECC causes the Wairarapa Eddy to develop (Chiswell and Roemmich, 1998). Outboard of Cook Strait, the warm ECC, which encompasses the south-bound Subtropical Front mixes with the colder, north-bound Southland Current, forming the Hikurangi Eddy (Heath, 1985; Stramma et al., 1995; Carter and McCave, 2002; Chiswell et al., 2015). These major gyres act to mix the oceanic water masses and redirect currents away from the subduction wedge back towards the DWBC (Fig. 3A; McCave and Carter, 1997; Stow et al., 2002; Carter et al., 2004).

**Fig. 3** (A) Bathymetric map illustrating the main structural features and physical oceanographic currents: East Auckland Current (EAUC), East Cape Current (ECC), Wairarapa Coastal Current (WCC), and Eddy (WE), Southland Current; Deep Western Boundary Current (DWBC); and the previously documented Hikurangi fan drift (Carter and McCave, 1994). Map compiled based on work by Barnes et al. (1992); Carter et al. (2002, 2004); Lewis and Pantin, (2002); Mountjoy et al. (2018). (B) Data coverage map illustrating the locations of 2D seismic surveys and wells investigated in this study of the Hikurangi Margin. Bathymetric data courtesy of NIWA.



## DATA AND METHODS

The data for this study includes: (i) high-resolution bathymetry, (ii) >15,000 line-kilometres of 2D seismic data, and (iii) limited wireline log data from three of the wells that penetrate the subduction slope (Fig. 3B). Bathymetric data (nominally at 100-metre grid resolution, but with areas of 25-metre resolution and backscatter imagery), accessible via the National Institute of Water and Atmosphere Research, New Zealand (NIWA), were used to examine the modern seafloor for sediment waves in order to identify areas of active bottom current reworking (*sensu* Wynn and Stow, 2002). The seismic dataset comprises six 2D seismic surveys covering the east coast of New Zealand, with open source data provided by New Zealand Petroleum and Minerals (NZPM) and newer data provided by WesternGeco (Table 1A). Analysis of the seismic data was carried out over a depth range of c. 0 – 4,000 metres across the margin, but was restricted to the relatively shallow subsurface. This was due to limited seismic resolution within the highly deformed pre- and syn-subduction stratigraphy, which precludes recognition of the geometries necessary for accurate drift interpretation (Fig. 2). Drifts were interpreted in the subsurface through the identification of diagnostic first, second, and third-order seismic features (see Faugères et al. 1999; Stow et al. 2002; and Smillie et al. 2018):

- First-order seismic elements describe the overall, large-scale architecture, external geometry, internal reflector character, and upper and lower bounding surfaces.
- Second-order observations describe the internal architecture of first-order elements, including the identification of medium-scale seismic unit shape, stacking pattern, and reflector terminations.
- Third-order elements describe the small-scale seismic facies variations, which are inferred to record changes in depositional processes and sediment types.

These diagnostic seismic elements are used to characterize drifts, interpret depositional or erosional conditions, assign facies, and infer bottom-water circulation and orientation. Depositional contouritic processes can be inferred to occur both independently of and in association with deposition of gravity process elements including channel-levees, lobes, and mass transport complexes (MTCs); erosional features include unconformities (i.e., local and regional major disconformable surfaces), contourite moats, furrows, and valleys (*sensu* Faugères et al., 1999; Hernández-Molina et al., 2008a, 2008b). The orientation of these depositional and erosional structures informs the interpretation of bottom current direction based on the migration of moats in relation to the Coriolis force, which deflects the current core along the relief, potentially causing reduced- or non-deposition (*sensu* Hernández-Molina et al., 2008a). Shallow underlying structural features such as faults and fractures were interpreted to examine the degree of sediment-structure interaction. To quality-check interpretations of possible buried or deformed drifts within the trench-slope basins horizon flattening of localized unconformable surfaces beneath candidate drifts was undertaken. Open access well data, including composite logs and final well reports, was provided by NZPM and the IODP from three penetrations (Fig. 3B, Table 1B) and used to assign facies and depositional events where possible. However, well coverage is limited over the study area, and the associated wireline logs and records of ditch-wall cuttings samples are incomplete, typically starting below the interval of interest. Following recognition of the principle drift types their distribution and areal extent along the margin was plotted to investigate the structural and oceanographic controls on their development.

**Table 1** (A) Seismic survey coverage and data quality of the Hikurangi Margin. Data courtesy of New Zealand Petroleum and Mineral (NZPM) and WesternGeco. (B) Well coverage and sampling intervals.

<b>A</b>	<b>Survey Name</b>	<b>Acquisition Year</b>	<b>Depth Interval</b>	<b>Access Provided By</b>	<b>Sample Interval</b>	<b>Vertical Resolution</b>	<b>Frequency</b>
	<b>MOBIL72</b>	1972	TWT (ms)	NZPM	4 ms	20 ms	20-30 Hz
	<b>IAE1</b>	1990	TWT (ms)	NZPM	4 ms	10 ms	40-50 Hz
	<b>05CM</b>	2005	TWT (ms)	NZPM	4 ms	12 ms	30-40 Hz
	<b>BRUIN</b>	2005	TWT (ms)	NZPM	4 ms	8 ms	40-60 Hz
	<b>PEG09</b>	2009	TWT (ms)	NZPM	4 ms	12 ms	30-40 Hz
	<b>PEG14</b>	2014	TVDSS (m)	WesternGeco	3 ms	15 m	0.04-0.08 m <sup>-1</sup>

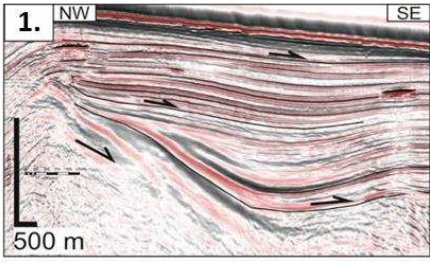
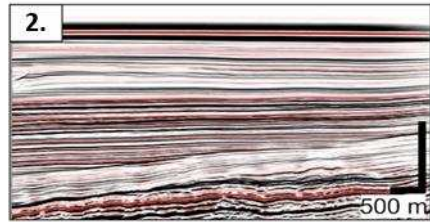

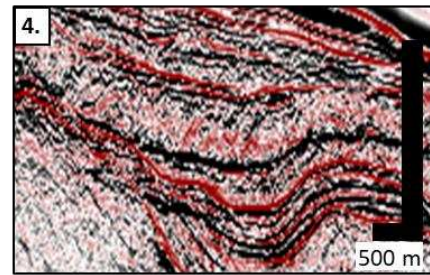
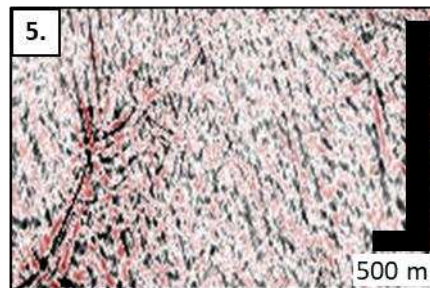
<b>B</b>	<b>Well Name</b>	<b>Operator</b>	<b>Year</b>	<b>Total Depth</b>	<b>Wireline Coverage</b>	<b>Core Interval Recovered</b>	<b>Data source</b>
	<b>Titihaoa-1</b>	Amoco NZ	1995	2741 m	600 m-TD	1997-2552 m; 2673-2670 m	Biros et al., 1995
	<b>Tawatawa-1</b>	Tap Oil Ltd.	2004	1560 m	231-1555 m	750 m -TD	Tap Oil Ltd. 2004
	<b>Hole U1519</b>	IODP	2018	640 m	0 m -TD	0-119.2 m	Saffer et al. 2018

## RESULTS

### Seismic Facies

The large-scale architecture and seismic facies associations of both contouritic and non-contouritic Hikurangi Margin sedimentary deposits can be defined using seismic data, some of which may be calibrated with well data. Five non-contouritic seismofacies are defined in Table 2 (modified after McArthur et al., 2019). These include muddy shelf clinothems, (hemi-) pelagic muds, mass transport deposits, turbidites, and seismic basement. The sixth, contouritic, seismofacies can be subdivided into individual drift types that are described in detail below.

**Table 2.** Seismic facies of the Hikurangi Margin. Images courtesy of WesternGeco.

Seismofacies (SF)	Amplitude and dimensions	Interpretation
	<p>Often high amplitude reflectors, which variably grade into and downlap strata, forming wedge shaped geometries, tens to hundreds of metres thick, and tens of kilometres in length. Well penetrations exhibit silty mudstones (see Fig. 4C).</p>	<p>Muddy shelf clinoforms stepping off the near-shore sections of the upper shelf-slope break (NW-SE). Various progradational and retrogradational degrees of development into the basin and the Cook Strait.</p>
	<p>Often high amplitude, laterally continuous, tens to hundreds of metres thick, 1,000s' to 10,000s' metres wide, with internally coherent reflectors. May onlap structural highs, and fill paleo-topography. Common on the subducting plate, but also in trench-slope basin fill.</p>	<p>These homogenous reflectors are interpreted to represent background, mud dominated, pelagic to hemipelagic sediments (<i>sensu</i> Vinnels et al., 2010), but could also include the distal dilute tails of turbidity currents.</p>
	<p>Chaotic fill of irregular packages tens to hundreds of metres thick, often 1000s' of metres wide. Rarely demonstrate coherent rafts of banded material, overlain by a blocky, irregular upper surface reflector.</p>	<p>These are interpreted to represent gravity-driven mass wasting events (MTCs) of variable composition, filling the trench slope basins within the inner subduction wedge (<i>sensu</i> Posamentier and Kolla, 2003).</p>
	<p>Alternating high and low amplitude packages of coherent reflectors of variable lateral continuity, typically hundreds of metres thick and thousands of metres wide. May occur in lenses or more sheet like, thickest in the core of sub-basins, whilst thinning and onlapping relief at the margins.</p>	<p>These are interpreted as alternating sedimentary packages of sand and mudstones filling basins in the form of turbidites, which may be filling channels, forming lobes or ponding in basins (<i>sensu</i> Prather et al., 1998; Kneller et al., 2016).</p>
	<p>Variable thickness below SF 1 – 4, often low to transparent amplitude, discontinuous and chaotic reflectors, penetrated by deep and shallow linear high and low amplitude (fluid anomaly) reflectors.</p>	<p>This seismic basement is interpreted as highly deformed pre-kinematic stratigraphy, composed of (meta)-sedimentary rocks exhibiting both thick and thin skinned faults (<i>sensu</i> Lewis and Pettinga, 1993; McArthur et al., 2019).</p>

## 6. Contourites

See Section 4.1 for detailed descriptions, interpretations and facies associations of the characteristic drift types found along the margin.

## Drift Types

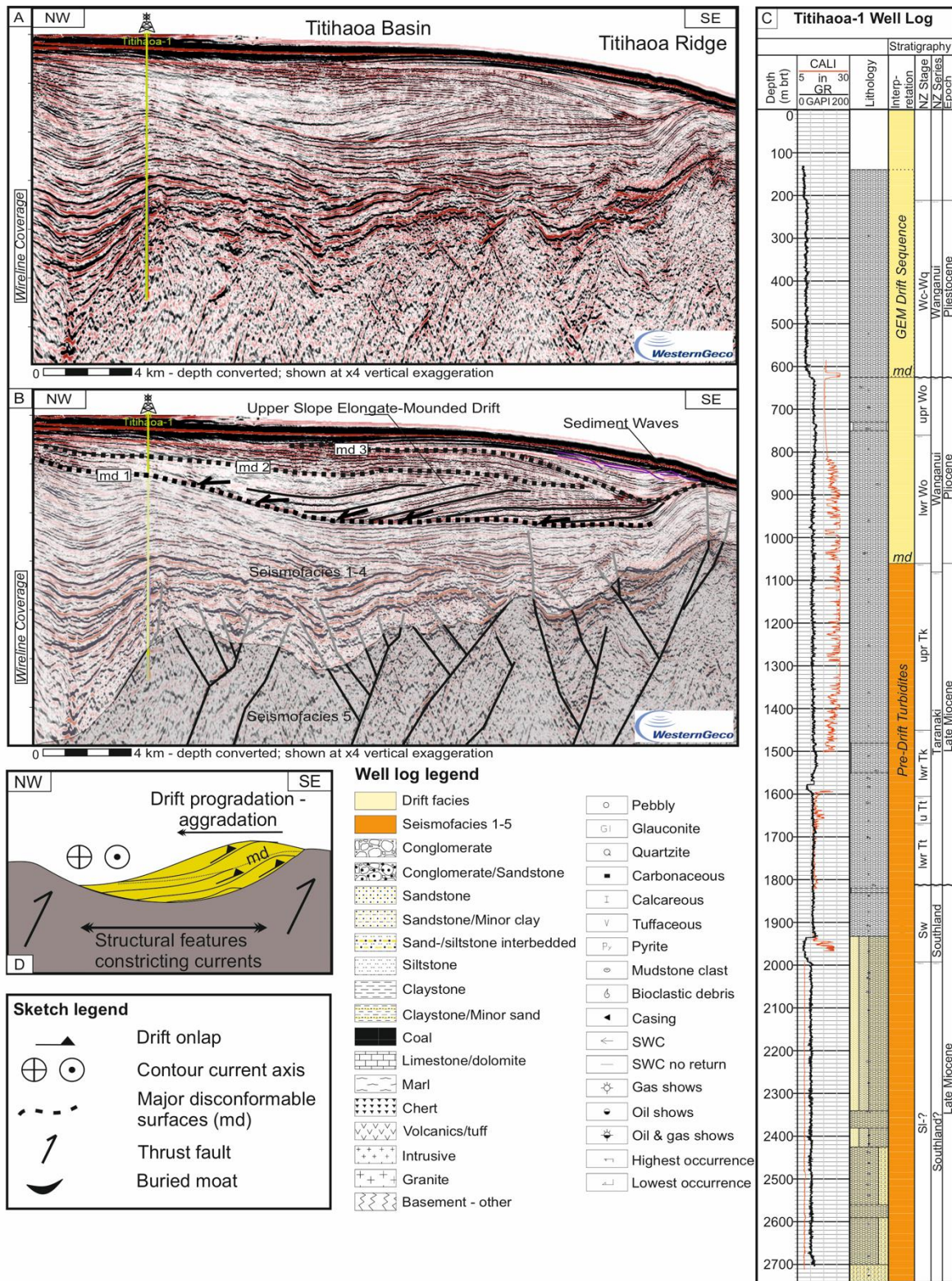
Analysis of the sub-surface dataset enables recognition of five contourite drift types along the submarine slope and trench of the Hikurangi Margin; these include examples from the mounded and sheeted categories (*sensu* Faugères et al., 1999; Rebesco et al., 2014), as well as a hybrid category (e.g., drifts representing the modification by contour currents of what are primarily gravity current deposits; *sensu* Shanmugam et al., 1993). The characteristic styles of drift architecture and geometry enable determination of the principal factors controlling drift type and composition (*sensu* Faugères et al., 1999; Hernández-Molina et al., 2008a, 2008b).

### *Giant Elongate Mounded Drift*

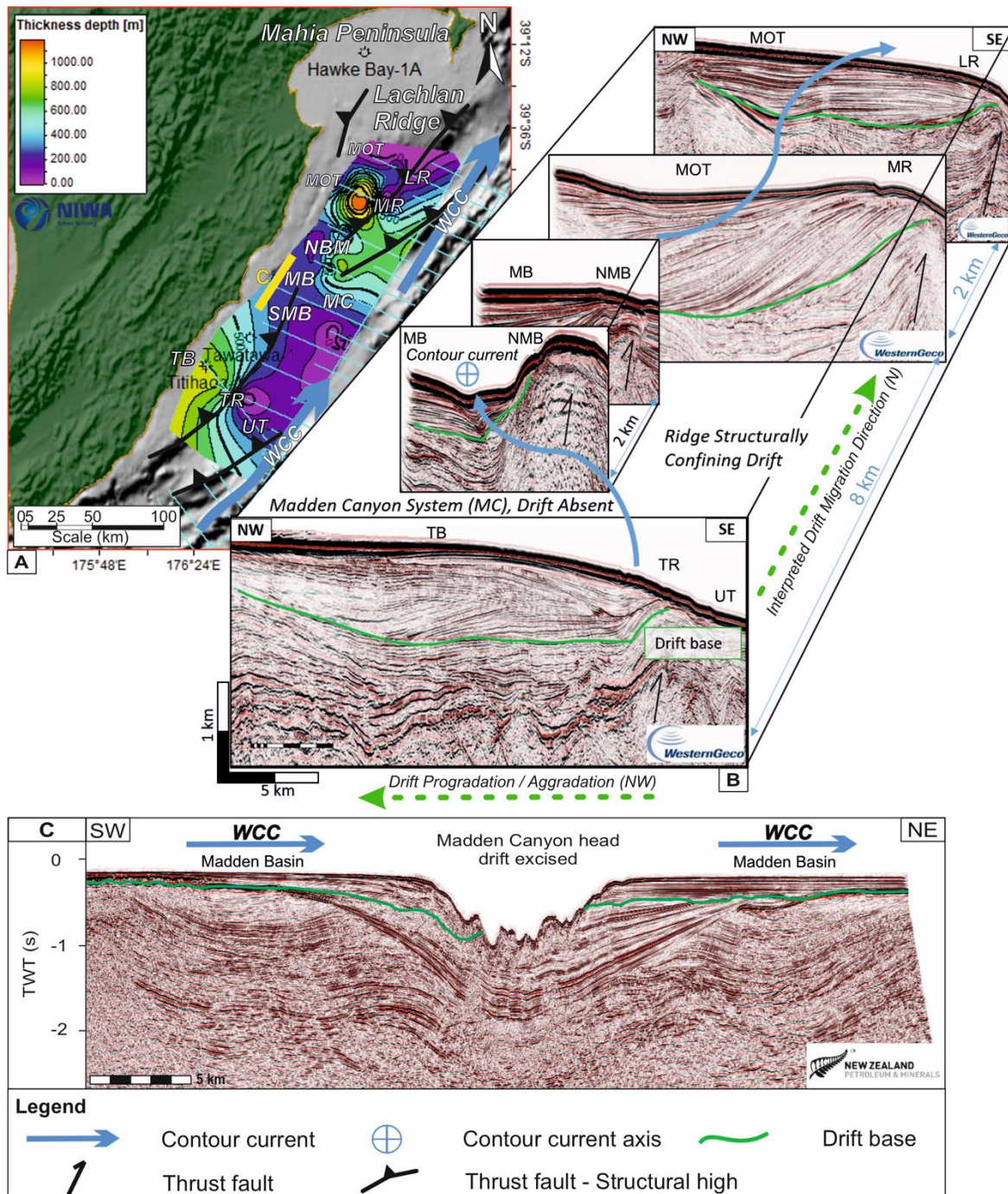
*Observations:* Examples of the giant elongate mounded drift type (GEM) straddle the continental shelf, shelf-slope break, and upper slope of the margin (Fig. 2) in water depths of 200 to 1,500 metres. To first order, GEM drifts form broad sediment packages, approximately 150 km long, 50 km wide, and up to 1,100 metres thick (Figs. 4 and 5). The internal architecture of the drifts is expressed as sub-horizontal reflectors, where dips steepen (up to 60°) prior to downlapping or onlapping older reflectors comprising SF 2-5. At the second order, the internal reflectors, characterized by major disconformable (md) surfaces, stack sigmoidally shoreward (to the NW) and parallel the strike of the Lachlan Ridge and Madden Banks (NE-SW). Internal facies are moderate-to-low amplitude, occasionally truncated by high amplitude erosional disconformities forming macro-scale wedges, with lateral incisions hundreds to thousands of metres wide. Data from wells Tawatawa-1 and Titihaoa-1 record an abrupt fining upward signature at the base of the GEM (Fig. 4C). Coarse-grained deposits at the base transition to overlying fine-grained (mudstone – dominated) facies that persist in the upper 1,000 meters of each well, essentially accreting from the Late Miocene through to the modern day (Crutchley et al., 2016).



*Interpretation:* The GEM drifts are interpreted from seismic geometries as an aggradational and progradational drift type; they migrate (towards the NW) along the zone bounded by the semi-buried upper slope of the subduction wedge and the back-limb of the downslope bounding thrust-cored ridge (Fig. 5). Although largely continuous along the upper slope, the drifts are cut in several locations by slope canyons, which may be fed by an along-slope sediment transport mechanism (McArthur and McCaffrey, 2019). Studies from passive margin settings document the GEM drift type to grow with enhanced rates of deposition (up to 20 – 60 cm kyr<sup>-1</sup>), adjacent to one or more localized high velocity currents (Faugères et al., 1999; Rebesco et al., 2014), whereas their deposition rates in convergent margins are less well constrained. Here, the GEM drift type is thought to record late Neogene deposition in thrust-generated accommodation, but thickness and evolution was influenced by intrabasinal structural growth and likely by subordinate eustatic sea-level variations (Carter et al., 2004). Specifically, in this location drift growth is interpreted to relate to the uplift of the large intrabasinal Lachlan Ridge and Madden Banks; the back-limb of these thrust-cored ridges formed accommodation space healed by contourite deposition during periods of vigorous bottom current activity. Major internal disconformities are thought to record intervals of non-deposition and erosion, which can possibly be attributed to sea-level variations, which likely control bottom-water circulation through the Mahia Strait and into Hawke Bay (Paquet et al., 2009). In both wells, the base of the drift coincides with the change from influxes of coarse-grained sediments, interpreted as gravity current deposits, to the fine-grained system, demonstrating that these drifts are composed primarily of mudstone (Fig. 4C).



**Fig. 4** (A) Non-interpreted and (B) Interpretation of the giant elongate mounded (GEM) drift located along the upper slope, shown with a vertical exaggeration of x4. Here the drift is penetrated by well Titihaoa-1. md = major disconformity. (C) Titihaoa-1 well log showing penetrated drift facies and biostratigraphic age boundaries, which show this drift to have been developing since the Late Miocene (modified from Biros et al., 1995). (D) Sketch of drift development in relation to structural features.



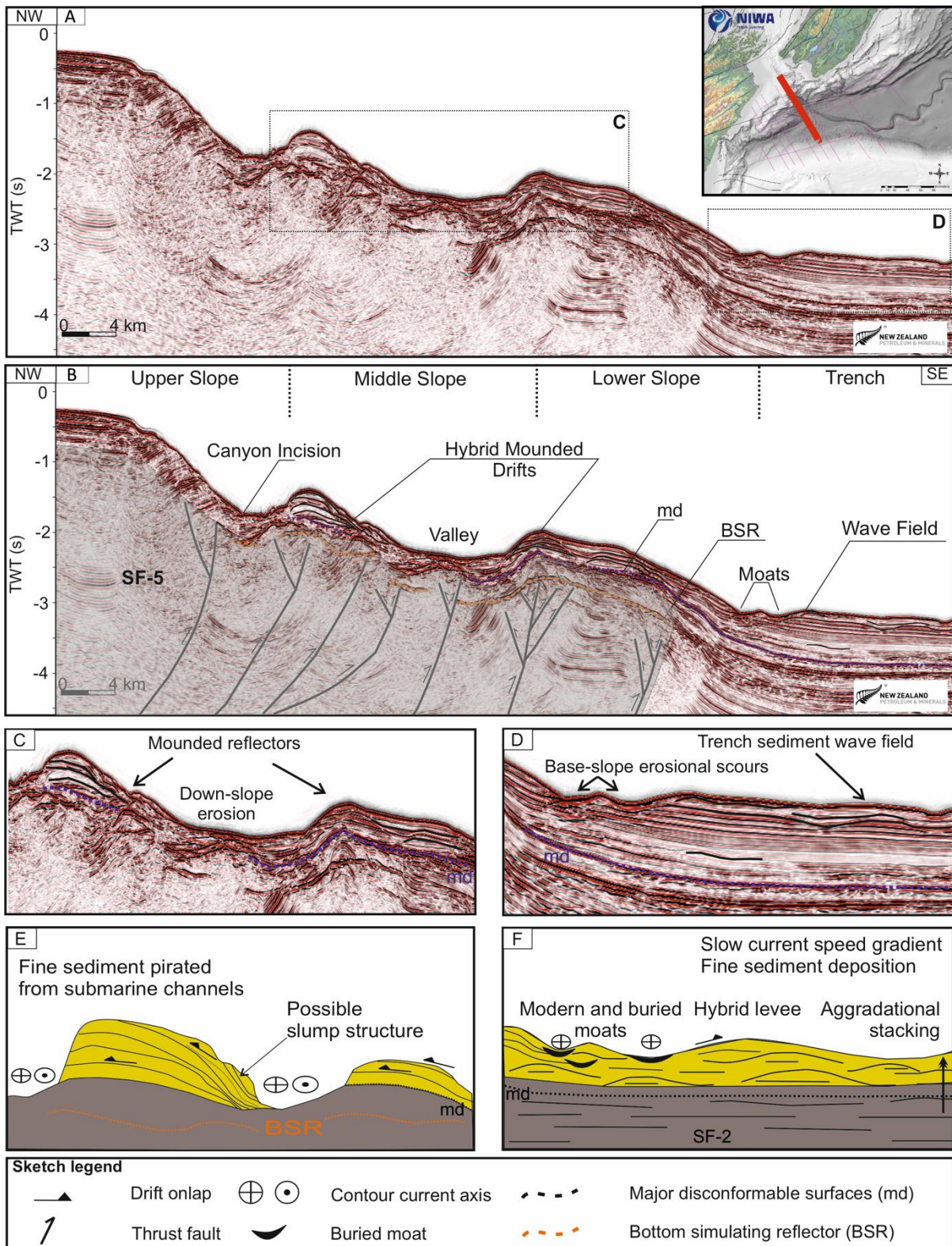
**Fig. 5** (A) Thickness map (TVDSS, metres) and (B) fence diagram of GEM drift, showing along-shore migration and inferred structural displacement of contour currents by the Lachlan Ridge and the Mahia Peninsula. Labelled structures: Lachlan Ridge (LR); Madden Basin (MB); Madden North and South Banks (NMB, SMB); Motuokura Ridge (MR) and Trough (MOT); Titihaoa Basin and Ridge (TB, TR); Uruti Trough (UT); and Wairarapa Coastal Current (WCC). (C) Cutting of the GEM drift by the Madden Canyon, seen on line Bruin-002 (yellow line on map). The seismic lines are shown at approximately the same scales and with similar vertical exaggeration. Bathymetry courtesy of NIWA; seismic data provided by WesternGeco and NZPM.

### *Mounded Hybrid Drift*

*Observations:* The mounded hybrid drift type is located along laterally discontinuous bathymetric highs of the upper-middle slope outboard of the Cook Strait and associated slope canyons (Fig. 6), in water depths of 1,000 to 1,500 metres. The overall geometry is gently mounded (20 – 10<sup>3</sup> metres long, <0.4 seconds (TWT) thick [c. 500 m]), whilst erosive features 1 – 2 km wide punctuate drift margins (Fig. 6B-C). Reflector stacking pattern is aggradational along the crests while thinning towards the margins or truncated by base-of-slope incisions, forming an upwardly-convex geometry (Fig. 6C). The seismic facies architecture consists of weak-to-transparent, semi-continuous reflectors, which downlap onto underlying reflectors of SF-5 (Fig. 6C). The drift mounds are detached from the upper slope by erosive features within the submarine canyon system. This drift type is not observed to be laterally continuous (Figs. 6C-D).

*Interpretation:* Its occurrence along relict canyon walls downstream of Cook Strait is interpreted to indicate that this drift type forms part of hybrid channel-levee systems; depositing currents are interpreted to incorporate components of both along-slope and downslope flow, and to carry sediments pirated from the slope channel network (Fig. 6E). The sediment transport regime associated with this hybrid drift type is here attributed to the strong semidiurnal tides along on the shelf in association with gravity-driven sediment influx to the trench (Mountjoy et al., 2014, 2018; Stevens et al., 2019). The upper slope channels promote high energy flow, such that major episodes of mass wasting and turbidity current influx transport shelf-derived, coarse-grained sediment to the trench, whilst largely incising and bypassing the slope (Mountjoy et al., 2009, 2014, 2018). Sediment passing through these conduits, particularly the component carried in suspension, is thought to be susceptible to pirating and contour current reworking, hence acting as the source for this drift type (e.g.,

Fonnesu et al., 2020). Although there are no well penetrations, the scale and wavelength of these drifts imply a fine-grained composition (Figs. 6D and F).



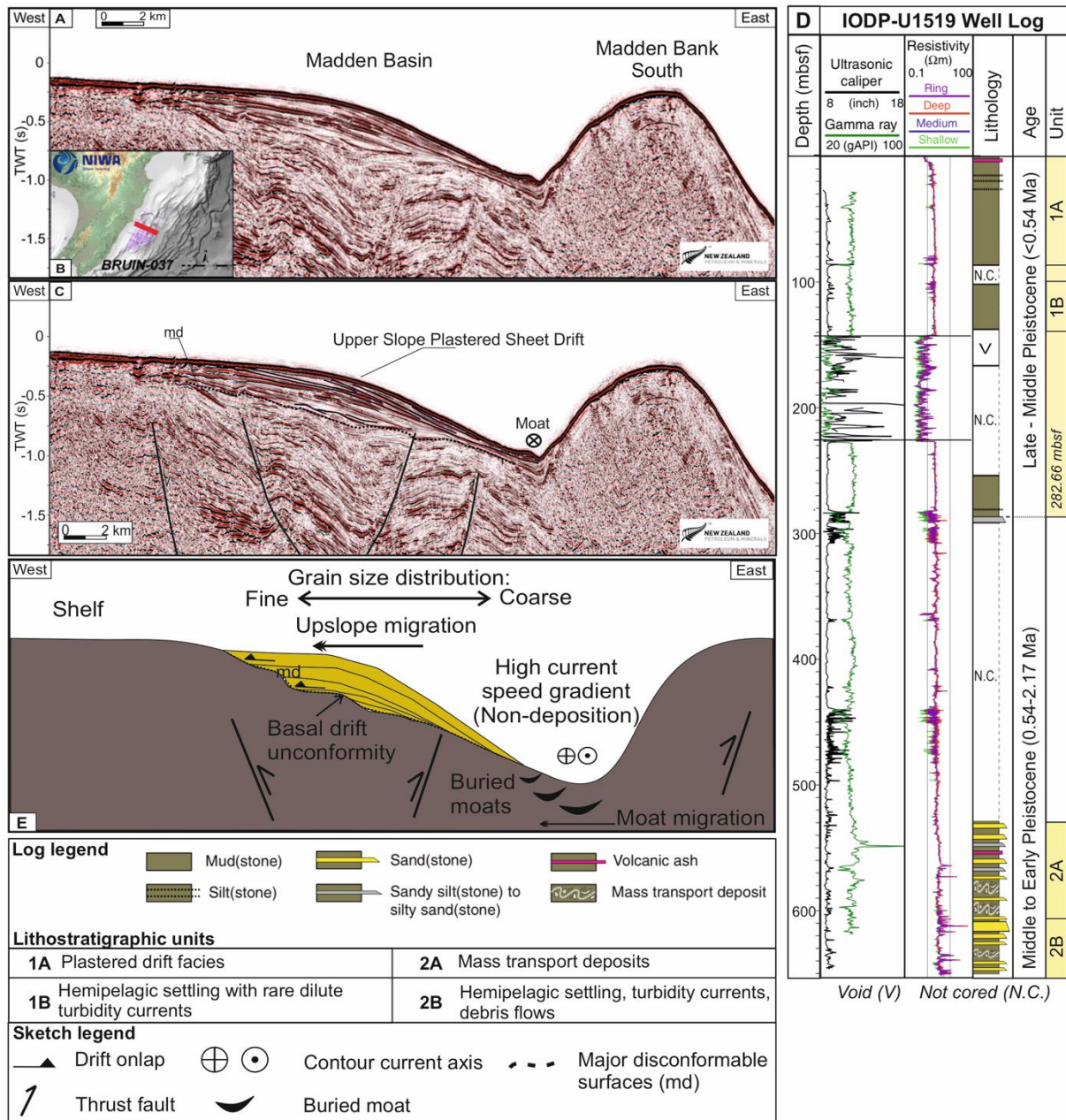
**Fig. 6** (A) Seismic data (line PEG09-13M1000) and (B) interpretation of hybrid-mounded drifts in a location proximal to Cook Strait, showing associated seismic facies (SF) and major disconformities (md); BSR – bottom simulating reflector. (C) Mounded reflectors with lateral truncation are interpreted to record the interaction between downslope and along-slope contour currents to form a hybrid drift system. The separated drift illustrates along-slope and upslope migration. (D) Sediment wave field within the abyssal plain trench comprising aggradational reflectors, interpreted to reflect interaction of bottom currents with the Hikurangi Channel – derived sediments. (E) Sketch of mounded drift development; (F) sketch of drift related sediment wave field with associated erosional and depositional features.

### *Plastered Drift*

*Observations:* The sheeted drift type blankets the upper slope domain in water depths of 500 to 1,500 metres, along the central and northern shelf-slope break (an area up to 300 km long and 8 km wide on this margin; Fig. 7). The overall geometry of these drifts is that of a thin veneer of reflectors (<0.5 sec (TWT), c. <600 m thick), which parallels the slope of seafloor topography. The internal architecture of these drifts comprises moderate-to-high amplitude, laterally continuous, sigmoidal to sub-horizontal reflectors overlying thrust-cored ridges of seismic basement (SF-5). Internally, seaward-dipping reflectors stack along the gentle slope and smooth the ridge topography (Fig. 7C). The drifts' internal facies transition to high amplitude reflectors at the upper and lower slope, where drifts thin and eventually terminate, often with an erosional lower contact (Fig. 7C). Data from the IODP well 375, hole U1519, records an overall fining upward signature through the drift, where coarser-grained deposits at the base transition to overlying fine-grained (mudstone – dominated) facies in the upper 300 metres, from the Pleistocene through the Holocene (Fig. 7D, Saffer et al., 2018).

*Interpretation:* This drift type records periodic episodes of progradation and aggradation along the upper slope domain of the subduction wedge (Fig. 7E). Multiple sediment sources are interpreted to interact with the plastered drift as the result of sediment pirating from shelf-attached submarine canyons and entrainment of unconsolidated hemipelagic sediments by along-slope bottom currents. As the ridge gradient becomes too steep for

turbidite deposition from dilute low-density gravity flows (i.e.,  $>9^\circ$ ), contourite processes dominate, forming drifts upon smooth, sloping topography (Hernández-Molina et al., 2008b; Preu et al., 2013). The basal high-amplitude reflector marks a significant unconformable surface, potentially relating to an earlier mass transport event or an erosional bottom current episode (*cf.*, Faugères et al., 1999). Based on the lack of evidence of a downslope MTC, the basal unconformity is interpreted to relate to the initiation of drift, where stronger bottom currents may have eroded the upper slope prior to deposition and upslope progradation. The drift represents a mixed flow regime recording where the contour current may be either actively depositing or eroding (Hernández-Molina et al., 2008b). Along the shelf, a gentle flow regime predominates, yielding net-deposition of fine-grained material, while the erosion-prone lower slope is dominated by a basal axial channel or contourite moat structurally pinned by the upper slope bathymetric highs (i.e., Madden Banks), potentially favouring the deposition of coarser grain sediments (Fig. 7E, Hernández-Molina et al., 2008b; Rebesco et al., 2014). IODP well U1519 records a change from influxes of coarse-grained sediments, interpreted as gravity current deposits, to the fine-grained system, implying that these drifts are composed primarily of silty mudstone (Fig. 7D, Saffer et al., 2018).



**Fig. 7** (A) Plastered drift, with location map of line Bruin-037 in B. (C) Interpretation, showing a major disconformity (md) possibly records the initiation of the drift, a period of an erosive bottom current regime (see text for discussion). Approximately 4x vertical exaggeration applied to accentuate depositional gradient of South Madden Bank. (D) IODP well log illustrating drift facies and Pleistocene to Recent age (modified from Saffer et al., 2018). (E) plastered drift model illustrating grain size distribution related to temporal bottom current regimes recorded by migration of buried moats.



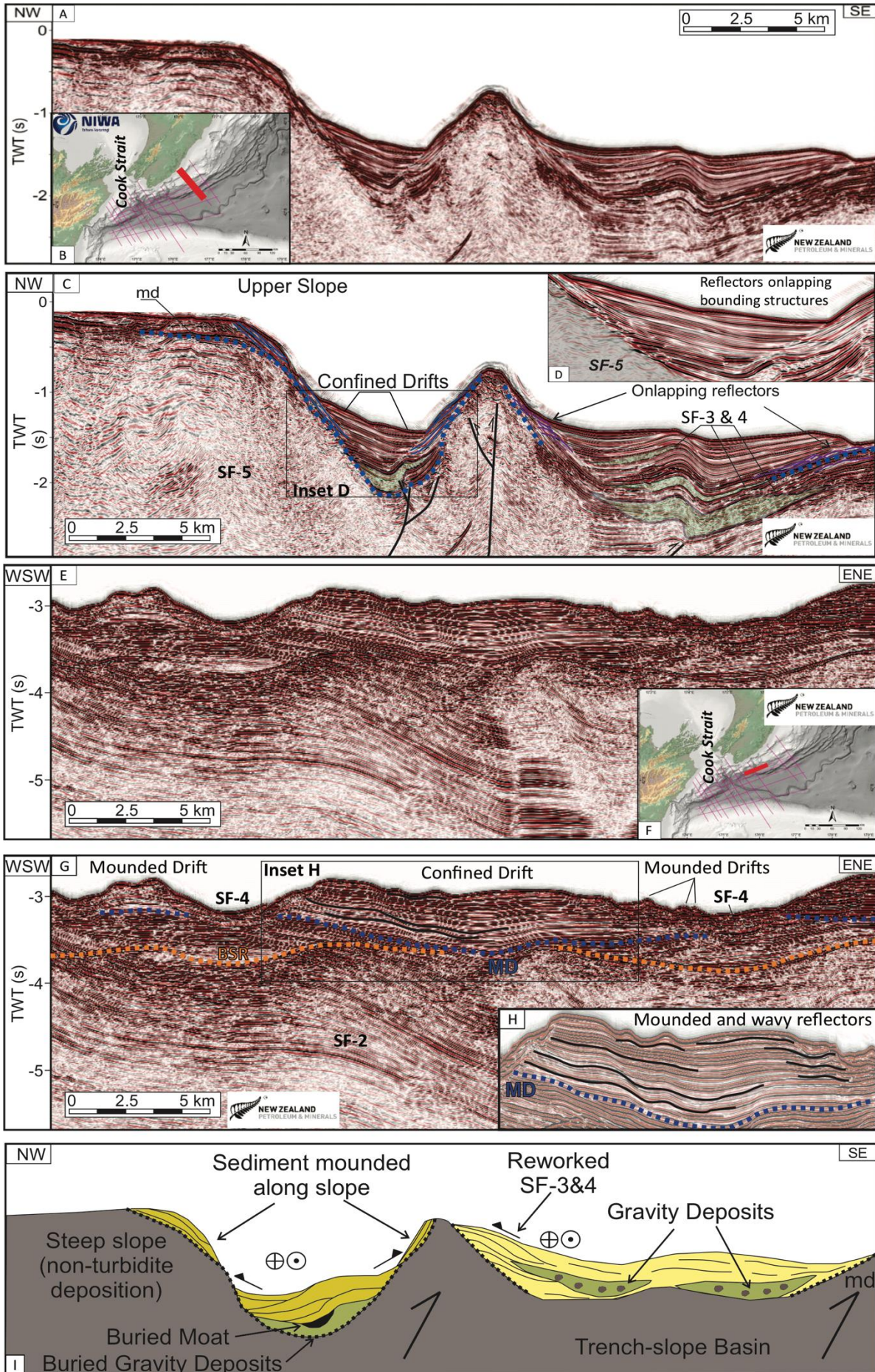
### *Confined Hybrid Drifts*

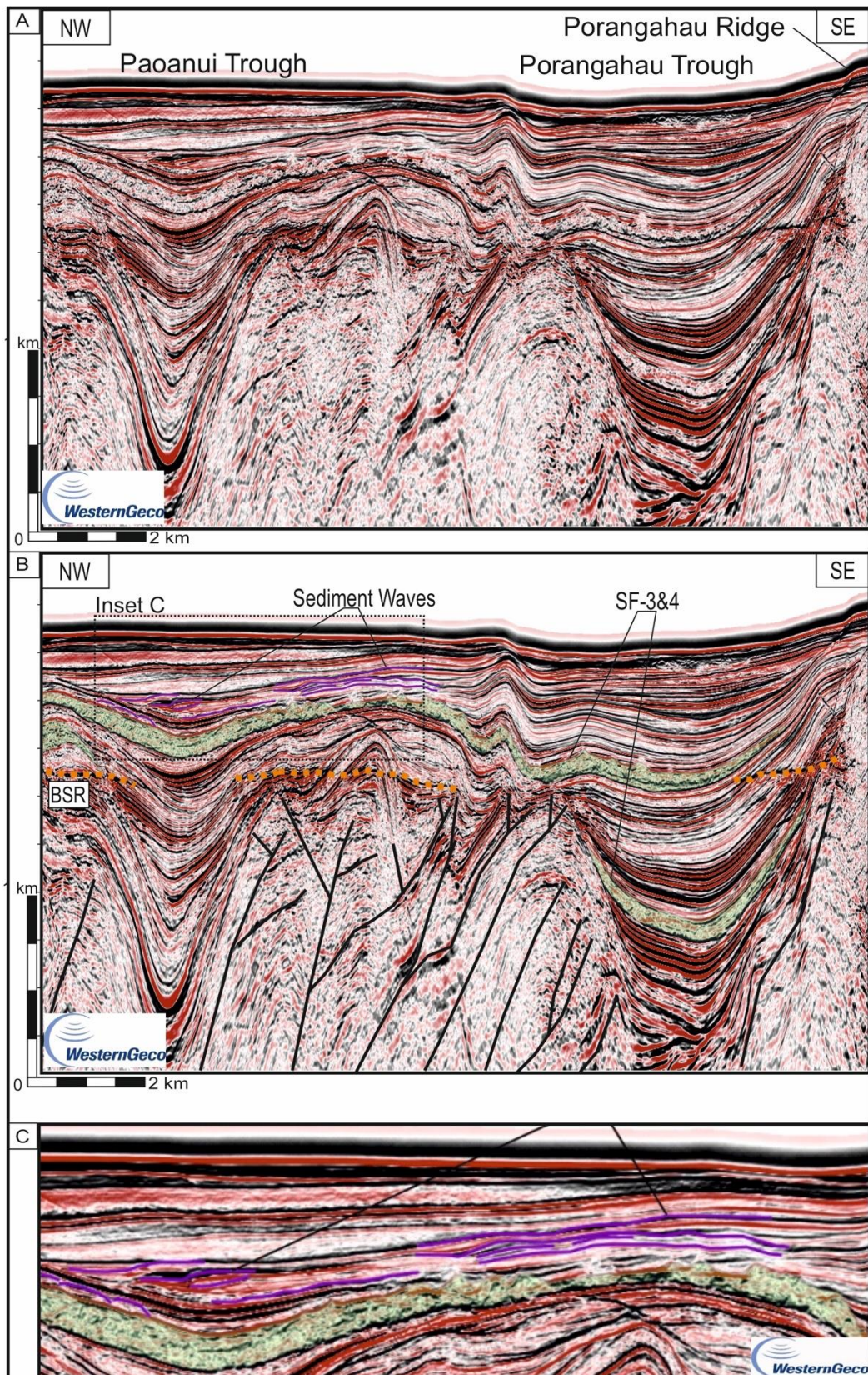
*Observations:* Confined drifts are located along the upper, mid and outer slope domains within narrow trench-slope basins comprising the interior of the subduction wedge. These drifts are largely discontinuous (10s – 1,000s of metres wide, <1,000 metres long), forming narrow lenses of sigmoidal reflectors within the shallow subsurface (<1.5 sec TWT, or <2,000 m TVDSS) (Figs. 8, 9 and 10). The external geometry of these drifts is characterized by the development of spatially discontinuous mounds, principally occurring adjacent to bathymetric highs and as sub-horizontal basin-fill (Figs. 8-10). The upper surfaces of these drifts are lenticular, with wavy, upwardly-convex surfaces where internal architecture is typically defined by sub-horizontal to wave-like reflectors (Figs. 8D, 8H and 9C). Internal reflectors stack via aggradation and progradation, whilst fanning towards the basin depocenter before terminating with smooth upper unconformable surfaces (SF-2) (Figs. 9C and 10C). Wavy, moderate- to-high amplitude internal reflectors onlap earlier basin-fill strata (of SF-3 and 4) or seismic basement (SF-5), albeit often separated by a high amplitude basal reflector (Figs. 8C-H and 9C).

*Interpretation:* Sediment for this drift type is interpreted to be sourced by downslope gravity currents, whose deposits are partially modified by contour currents actively eroding and redepositing within the trench-slope basins (e.g., Rebesco and Stow, 2001). The interaction between the bathymetry and the along-slope flow of bottom currents spatially controls the degree of drift elongation and distribution. The walls of the thrust-cored ridges confine the drifts' lateral extension; the predominant migration direction is down-current and along the slope gradient. The drift architecture may transform up the lateral slope gradient to a mounded form (Figs. 8G and I; *sensu* Faugères et al., 1999, Juan et al., 2018). Gravity currents and channel-feeder systems develop turbidite channels, lobes, and MTCs within these basins, and act as the siliclastic source to the otherwise sediment-starved outer slope basins (McArthur et

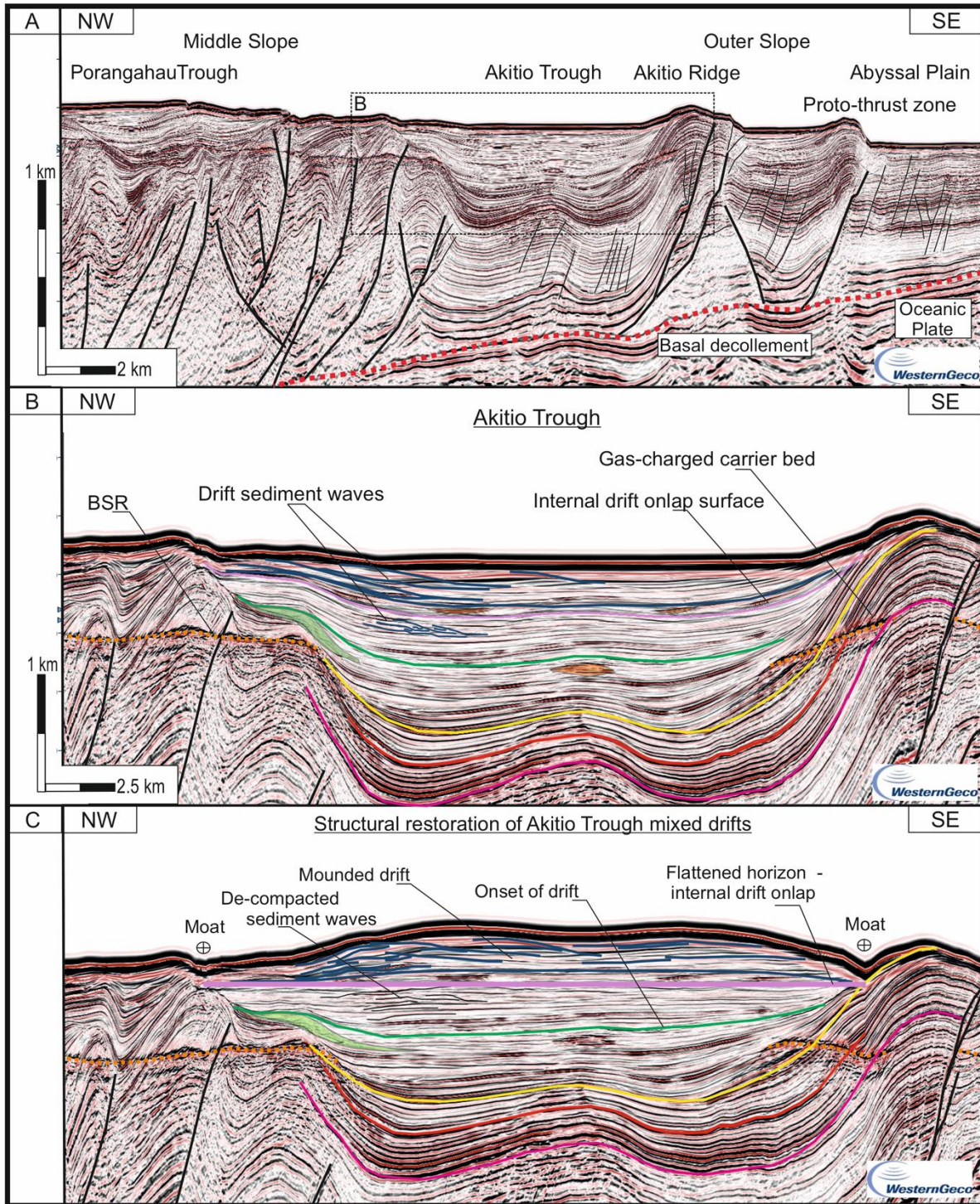
al., 2019). Within the host trench-slope basins, there is likely a process interplay between contour currents and gravity currents modifying both turbidite and contourite morphology. Structural restorations of a lower slope basin reveal possible multiple episodes of contourite reworking in the deeper sections of what were presumably relatively flat-lying basin-fill (Fig. 10). These drifts are interpreted to form between periods of uplift and mass transport when contour currents rework basin-fill facies, primarily evidenced by asymmetric sediment wave geometries that drape thrust ridges and prograde into the basin depocentre along the trough axis (Figs. 9C and 10B). Although no wells penetrate this drift type, the seismic facies imply a fine-grained composition. Along-slope currents are interpreted to clean and sort these gravity-sourced sediments along the uplifted margins of the trench-slope basins, to form narrow zones of fine-grained drifts (Fig. 8-10).

**Fig. 8** (A) Seismic in-line PEG09-23P1078 located proximal to Cook Strait (B). Seismic interpretation (C) of confined drift deposits and (D) enlargement of confined drift (note different vertical exaggeration); mounded reflectors onlap underlying basal unconformity (see text for discussion). (E) Seismic cross-line PEG09-02M1000, which runs along strike of the Pukehoko Trough (F). (G) Interpretation of line (E), with inset enlargement (H) showing the strike character of the confined drift (note different vertical exaggeration); here mounded reflectors are seen to terminate on the underlying basal unconformity and wavy reflectors are seen to decrease in amplitude away from the seismofacies 4 (SF-4) infilled slope channels. (I) Confined-mounded drift model illustrates the impact of turbidity current – contour current interactions (see Fig. 7E for key). SF – seismic facies; md - major discontinuities; BSR – bottom simulating reflector.





**Fig. 9** (A) Seismic section through the mid-subduction wedge, Paoanui-Porangahau Troughs. (B) Hybrid confined drift interpretation, where contour currents interact with gravity-driven sediment filling the trench slope sub-basins. (C) Enlargement, illustrating large scale sediment waves (1.2 km wavelength, 10s' m amplitude), evidence for contour current reworking the sediment ponded on top of MTDs (SF-3) and turbidites (SF-4).



**Fig. 10** (A & B) Seismic line transecting the Akitio Trough. (C) Hybrid confined drift de-compacted using horizon flattening of basal onlap unconformity (SB) of shallow sediment waves. Proxy restoration illustrates possible episodes of gravity-driven basin-fill deposition are followed by contourite reworking, as evidenced by sediment waves and progradational clinoforms, and characteristic mounded drift morphology.

### *Hikurangi Trench Hybrid Drifts*

*Observations:* Within the Hikurangi Trench, in abyssal water depths c. 2,500 m, large scale sediment waves (*sensu* Carter and McCave, 1994; Lewis and Pantin, 2002) are observable on overbank areas adjacent to the left-hand (NW) margin of the trench-axial Hikurangi Channel (Fig. 11). They are best developed outboard of outer bends, in areas downstream of the bend apices (i.e., some 30° around the bend; see bends *a* and *c* on Figs. 11B and C); here the crests of the principal wave sets are arcuate, and convex predominantly to the N or NNE. The sediment waves are characterized by wavelengths >2 km and heights of 10s of metres; both wavelength and heights diminish away from the channel. In cross section the waves are asymmetric (Figs. 11D and E) and although complex, the steeper sides are generally facing and hence accreting towards the channel (Figs. 11E and F); buried wave fields, exhibiting internal seismic facies comprising moderate-to-transparent wave-like reflectors intercalated with flat, parallel reflectors (SF-2), generally show the same sense of accretion.

Bathymetric surveys acquired in the trench in 2013 generally document relatively abrupt lateral transition from the Hikurangi Channel margins to overbank areas. An exception is a channel reach some 40 km long that starts c. 5 km upstream of the apex of bends *a* and finishes c. 5 km upstream of the apex of bend *b* (Figs. 11A and B) in which the transition is smooth. Abrupt transitions are characterised by relatively sharp inflexions from inner channel to overbank areas and are associated with the common presence of lateral gullies on the channel walls; smooth transitions are characterised by progressive inflexions from inner channel to overbank areas associated with relatively smooth, non-gullied channel walls (Figs. 11A and B). In a bathymetric survey acquired immediately after the Kaikōura earthquake and seismically triggered turbidity current of November 2016 (Mountjoy et al., 2018; Fig. 11C) channel to overbank transitions in the 40 km reach that was smooth in the 2013 survey are seen to have become abrupt. New intra-channel gullying has cut back into overbank areas, such that

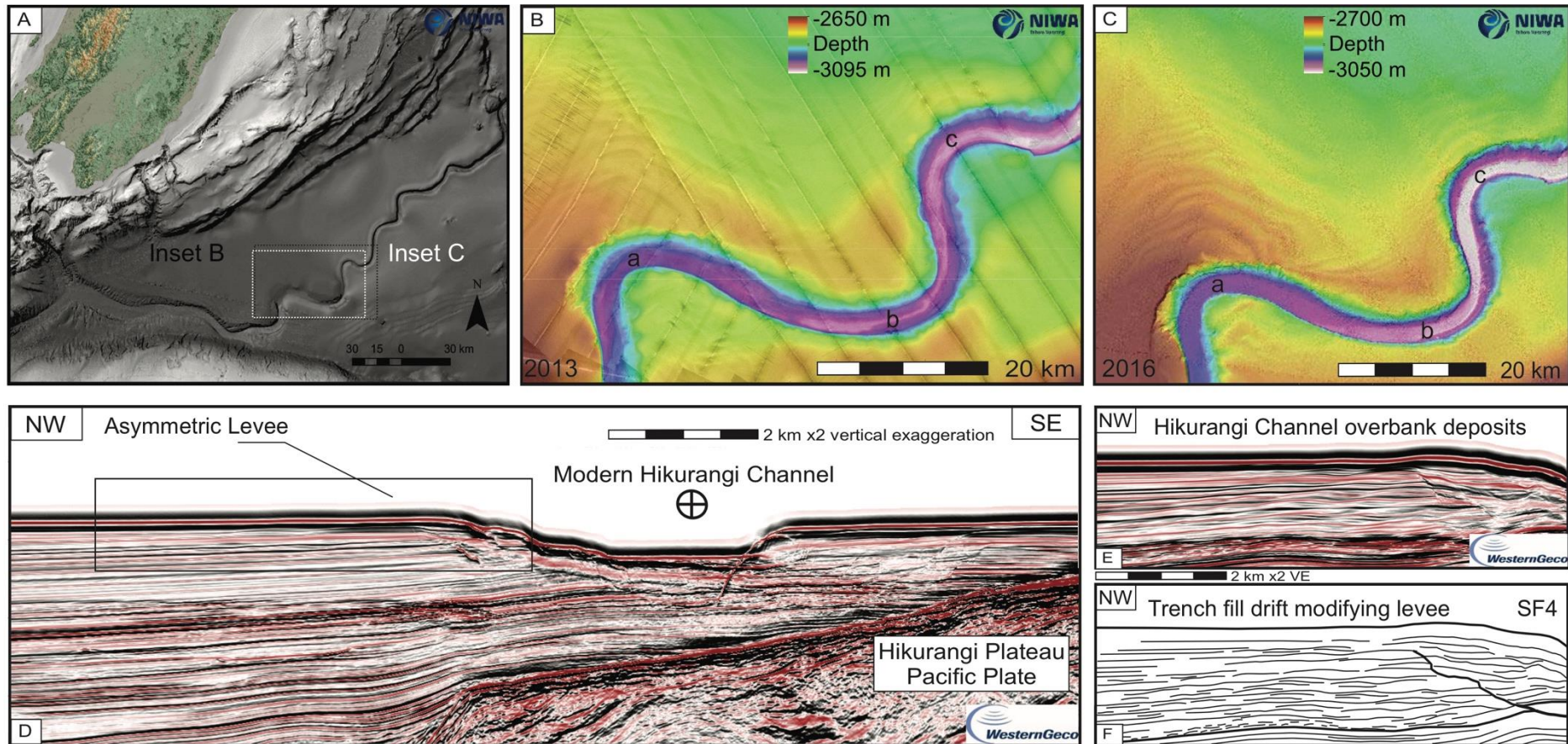
laterally-coalesced gully head scarps collectively define a sharp intra- to extra-channel transition that is particularly evident on the outer bend of channel *a* (Fig. 11C). The overbank wave field also appears more clearly defined in the 2016 data.

*Interpretation:* Because they form preferentially on outer bends of the Hikurangi Channel, the abyssal sediment waves (*sensu* Carter and McCave, 1994, Lewis and Pantin, 2002) are interpreted to result principally from flow-stripping of the upper parts of channelized turbidity currents onto overbank areas (Migeon et al., 2006; Wynn and Masson, 2008). Based on their amplitude and wavelength these sediment waves are interpreted to be composed primarily of mud, with minor amounts of silt and very fine sand (*cf.*, Wynn and Stow, 2002). On the assumption that wave crests form perpendicular to the current direction these unchannelised flows appear to disperse approximately northwards on the left-hand flank of the channel (Figs. 11B and C). However, the resultant wave forms generally accrete and migrate towards the channel, where wave crests steepen (*cf.*, Wynn and Masson, 2008). Although such a sense of accretion may indicate bottom current modification of the overbank deposits (e.g., Wynn and Masson, 2008, *cf.*, Fonnesu et al., 2020), similar growth of overbank waveforms towards a parental channel may also form due to turbidity current activity alone (e.g., Normark et al., 2002). Nevertheless, the inferred passage of a bottom current through the wave field and across the channel (see below) and changes to the wave field following the 2016 turbidity current indicate that the overbank sediment waves are likely hybrid features.

Although the downstream change from abrupt to smooth channel margins seen in the 2013 Hikurangi Channel bathymetry data could be associated with a turbidity current erosion limit, this interpretation cannot explain the re-establishment of abrupt margins some 40 km further downstream (Fig. 11B; Dorrell et al., 2019). Furthermore, in bathymetric data acquired after the 2016 Kaikōura earthquake, abrupt lateral transitions become evident in the reach that was formerly smooth (Fig. 11C). The earthquake-generated turbidity current flowed through

bends *a* to *c* and onward for at least several hundred km (Mountjoy et al., 2018). Such long-travelled seismogenic turbidity currents likely recur on average every 140 years (Mountjoy et al., 2018); the post November 2016 data indicate that these flows erode abrupt channel to overbank lateral transitions. It is inferred, therefore, that the smooth lateral transitions observed in the 2013 data likely developed between turbidity current events. We propose that this smoothing could be consistent with bottom current activity, and that the 40 km reach along which it occurred might represent the zone where a bottom current crosses the Hikurangi Channel (Fig. 12). In this scenario, through some combination of erosion of the sharp lateral scarp and of infill of channel wall gullies, the bottom current likely smoothed an abrupt, erosional channel profile sculpted by an earlier turbidity current, modifying the overbank wave field en route. Further study is required to confirm this interpretation.

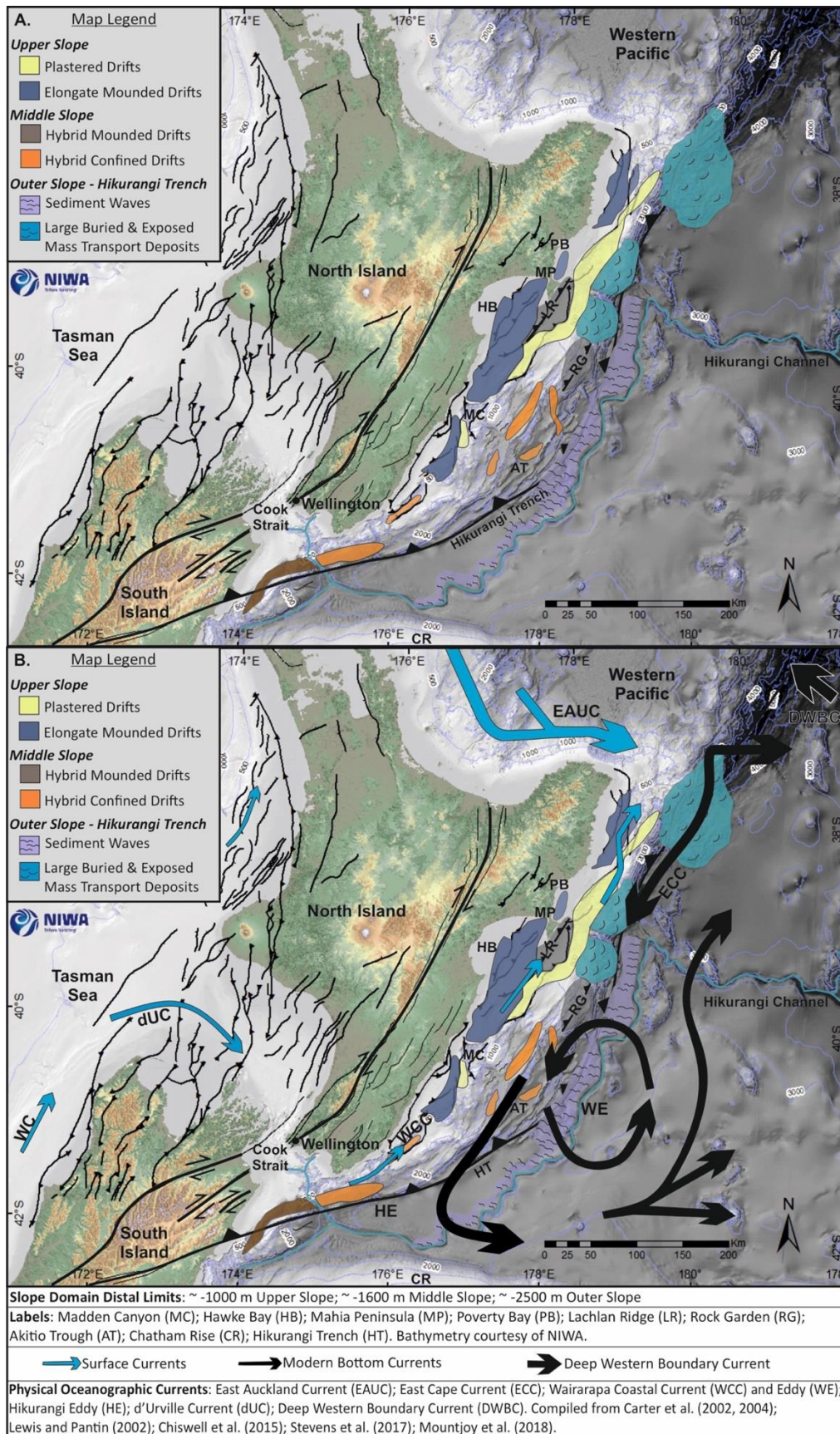




**Fig. 11.** (A) Location map of seafloor expression of the Hikurangi Channel and its overbank in the Hikurangi Trench. (B) Compilation of multibeam bathymetry (25 m grid) and backscatter data collected across three bends (a,b and c) of the Hikurangi Channel and overbank, collected by NIWA in 2013. (C) Detailed morphology of the three bends and overbank material immediately after the 2016 Kaikōura event, modified from Mountjoy et al., (2018). (D) Seismic cross-section showing sediment waves on the left bank levee to the channel, seismic line is within the inset boxes. (E) Inset seismic section illustrating variations in levee and overbank depositional style and seismic expression, to the left of seismic facies 4 (SF4) channel fill. (F) Channel-related trench-fill drift interpretation of sediment waves, note a complex alternation of lee face orientations, with a dominant direction to the SE, but with some larger waves to the NW. Seismic data courtesy of WesternGeco.

### **Distribution Mapping of Contourite Drifts**

Mapping the limits and occurrences of drift types illustrates the distribution of contourites along the Hikurangi Margin (Fig. 12A). The central to northern shelf and upper slope shows the GEM and plastered drifts trending parallel to the coast and along large structural ridges. The middle slope records a spatially discontinuous trend of hybrid drifts, some of which cross-cut bathymetric highs, but are typically confined within individual trench-slope basins (Fig. 12A). Contourites and gravity-driven deposits are also discontinuous along the margin in areas proximal to narrow upper slope basins and the network of submarine canyons (i.e., proximal to the Madden Canyon and Cook Strait canyons) and large bathymetric ridges (i.e., the Rock Garden). A broad sediment wave field characterizes the subduction trench on the left hand margin of the Hikurangi Channel (Fig. 12A), at least portions of which appear to be modified by bottom currents. The combined roles of structure and oceanographic currents are discussed below to investigate the controls of drift distribution along this convergent margin.



**Fig. 12** (A) Distribution map of different drift types identified along the Hikurangi Margin. (B) As A, but with orientations of modern oceanographic currents (Fig. 3A) superimposed.

## DISCUSSION

### Controls on Distribution of Contourites on Convergent Margins

This study reveals the hitherto undocumented presence of contourite drifts along the Hikurangi subduction margin. Although fundamentally reliant on the presence of bottom currents, a series of additional controls on the drift formation and distribution can be inferred, based on methods of assessing the interaction of oceanographic currents with seafloor relief developed in other settings (i.e., Stow et al., 2008; Chen et al., 2014; Ercilla et al., 2016; Juan et al., 2018). Contour currents documented around the Hikurangi Margin include the Deep Western Boundary Current (Stow et al., 1996; Stickley et al., 2001; Carter and McCave, 2002; Carter et al., 2004), the East Cape Current (Warren, 1981; Carter and McCave, 1997; Chiswell and Roemmich, 1998), the Wairarapa Coastal Current (Chiswell and Roemmich, 1998) and the currents and eddies arising from their interaction (Fig. 3A). Because oceanographic currents such as these may be accelerated when passing through bathymetric constrictions along the margin (*sensu* Hollister and McCave, 1984; Reed et al., 1987), current orientations with respect to slope and trench bathymetry were investigated to assess whether linkages could be made based upon the observed spatiotemporal evolution of drift distribution patterns (Figs. 12 A and B).

#### *Oceanographic Distribution Controls*

Factors recognised to influence drift distribution include bottom current strength (and any temporal variations) and different water mass properties (Heezen et al., 1966; Hollister and Heezen, 1972; Reed et al., 1987; Rebesco et al., 2014). Variations in oceanic stratification in terms of density (i.e., related to temperature and salinity), and in oxygenation in proximity to the continental slope are known to be associated with different water masses (e.g., Argentine margin [Preu et al., 2013]; South China Sea [Chen et al., 2014]; Gulf of Cadiz [Hernández-Molina et al., 2014]; Alboran Sea [Ercilla et al., 2016]; Mozambique [Fuhrmann et al., 2020]). Through linking prior mapping of bottom currents to observed depositional and erosional

features this study attempts to correlate drifts with the physical properties of specific water masses and the boundaries between them (*sensu* Preu et al., 2013; Rebesco et al., 2013; Hernández-Molina et al., 2014).

Although the current study incorporates what data there is from modern ARGO oceanic floats and from limited seasonal oceanographic datasets, little change in density with depth is documented (Chiswell et al., 2015; ARGO, 2019; Stevens et al., 2019). Temperatures of the different water masses taken from profiles recorded along the Chatham Rise indicate a possible correlation between the abyssal drift types and the Lower Circumpolar Deep Water (LCDW) and the Pacific Deep Water (PDW) masses, which feed the Deep Western Boundary Current ( $16.0 \pm 11.9$  Sverdrups [Sv]) outboard of the slope (Carter and McCave, 2002; Chiswell et al., 2015). However, the relatively simple modern oceanic stratification cannot solely account for the variety and complexity of drift types seen on this margin. Further, the influence of temperature and salinity variations on drift formation is dependent on variations in current strength of bottom water masses, which is still debated to vary temporally, such as when Antarctic Bottom Water or Antarctic Circumpolar Current is strongest, i.e., during interglacials (Ledbetter, 1984; Pudsey and Howe, 1998), interglacial – glacial transitions (Ledbetter, 1986; Masse et al., 1994) or glacial maxima (Pudsey and Howe, 1998). Regardless of temporal changes in current strength and orientation, a first-order association of drifts and their parental currents can be made. Thus, drifts forming along the outer slope and trench of the margin are associated with deep-water masses ( $> c. 2,500$  m), i.e., the DWBC, PDW, and LCDW (Fig. 12B; Ivchenko et al., 1996; Chiswell et al., 2015). In contrast, the warmer surface currents (i.e., Wairarapa Coastal Current [c. 1,000 m] and East Cape Current [c. 2,000 m]) are associated with shallower drifts forming along the shelf and upper slope of the margin (Fig. 12B; Carter et al., 2004). Seasonal bottom current activity such as benthic storms and eddies (e.g., Wairarapa and Hikurangi eddies), which act to mix the various water masses along the margin,

may be associated with the discontinuous drift trend proximal to Cook Strait (*sensu* Stow et al., 2008; Chen et al., 2014, 2019).

#### *Structural Controls on Drift Distribution*

A key control on drift distribution along the Hikurangi Margin is likely to be the structural variation of the actively evolving subduction wedge, which is inferred to locally channelize, block, and deflect bottom current pathways (Fig. 13). Based on the significant structural and morphological variability of the subduction wedge, the distribution of drifts are categorized by slope domains based on water depth, in order to associate drift types with their respective bottom currents (*sensu* Reed et al. 1987). Recognised domains on the Hikurangi Margin include: (i) the upper slope (c. 200 – 1,600 m), (ii) the mid-outer slope (c. 1,600 – 2,500 m); and (iii) the abyssal trench (c. >2,500 m).

On the upper slope, long-shore drift and wind-driven contour currents (i.e., Wairarapa Coastal Current) transport terrigenous and marine sediments along the shelf-slope break, here defined by the thrust-cored bathymetric highs (Fig. 12B; Carter and McCave, 2002; Carter et al., 2004). The GEM drifts are thought to record periodic growth and along-shore migration during Plio-Pleistocene to Recent glacial episodes. Rising and falling sea level, in combination with ongoing structuration, likely caused periods of stronger bottom currents, facilitating redistribution and deposition of sediments along the back-limb of intrabasinal structures, such as the Lachlan Ridge (Carter and McCave, 2002). The growth and thickness of GEM drifts vary according to the spatial variations in the degree of inferred basin-bounding and intrabasinal structure uplift and potentially sea-level fluctuations. Areas of increased drift thickness are attributed to prolonged duration of shallow contour currents undergoing net-deposition into areas of growing accommodation, whereas areas characterized by decreased thickness (not including drift margins or areas incised by submarine canyons) are associated with areas of local uplift.

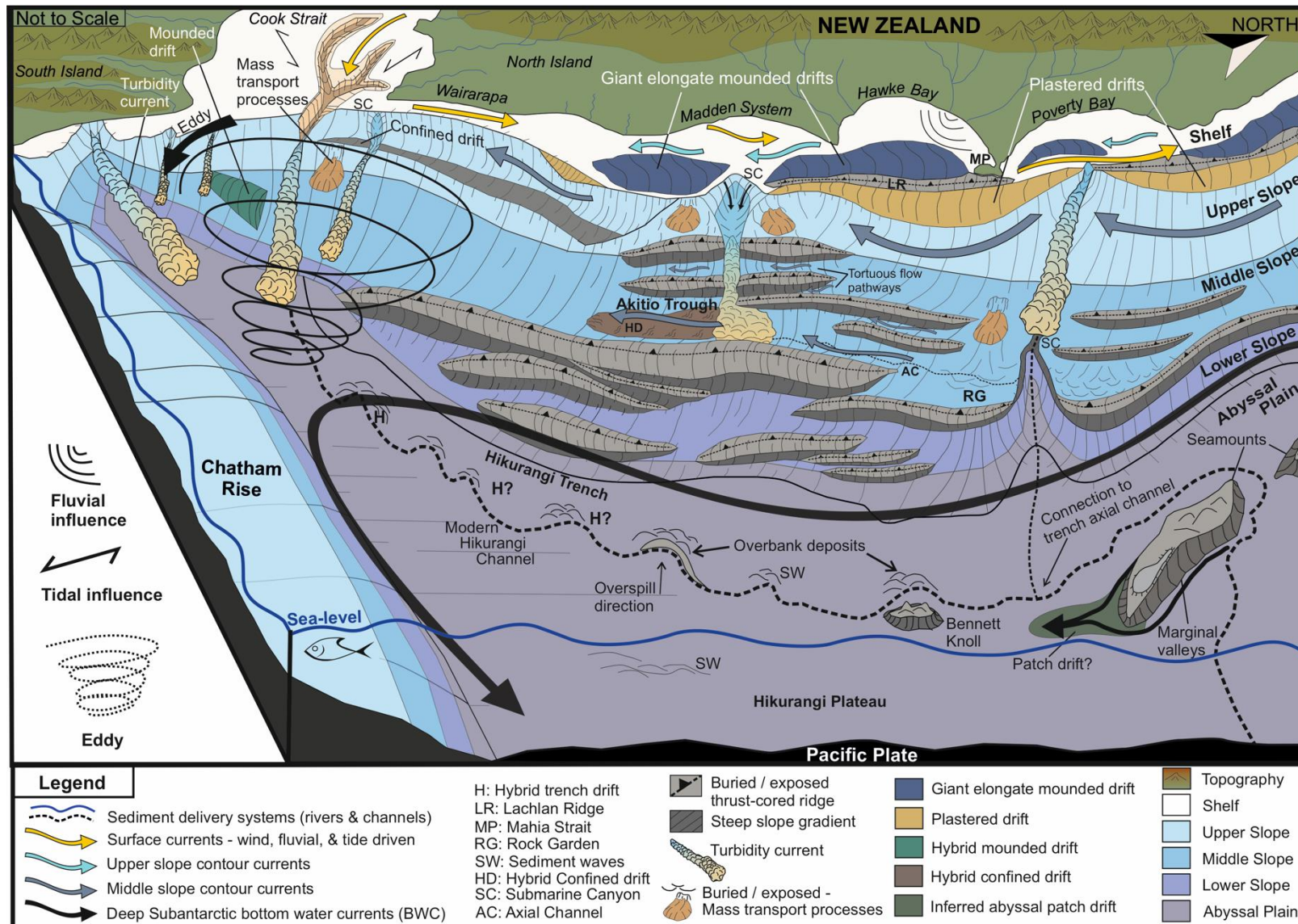
The growth of plastered drifts is associated with the deflection of shallow contour current flow along the upper slope. The periodic filling of the upper slope accommodation may also be associated with the construction of the plastered drifts, as bottom currents become reoriented along the shelf-slope break (e.g., Preu et al., 2013). The intermittent reorientation of these upper slope contour currents may possibly relate to the tectonic reconfiguration of Zealandia during the Neogene, and associated opening, migration, or occlusion of contour current pathways (Carter and McCave, 2002; Trewick and Bland, 2012).

The mid-slope domain of the margin shows drifts that cross-cut topography whilst interacting with gravity current deposits, involving the development of a tortuous style of bottom current conduit (Fig. 13). Within the trench-slope basins, the actively evolving thrust-cored ridges may locally constrict or block bottom currents resulting in the development of spatially-discontinuous hybrid drifts (Fig. 12). These deposits may record the interaction between bottom currents and gravity-driven basin-fill sediments, where present (e.g., Gong et al., 2013). Drifts forming in the relatively flat-lying trench-slope basin depocentres are laterally heterogeneous, showing modification towards basin margins (Figs. 9 and 10). These mid-slope drifts do not have a ready counterpart in classical drifts studies from passive margins in which drifts preferentially occur along submarine slopes (Preu et al., 2013; Rebesco et al., 2014). The variability of internal drift architecture may be associated with temporal variations in the strength of bottom currents, where periods of eustatic lowstands and glacial episodes increase bottom current strength and thermohaline overturn (*sensu* Faugères et al., 1999; Stow et al., 2008, 2018). However, internal drift heterogeneity may also reflect the opening and closing of bottom current conduits associated with the progradation and evolution of the thrust-cored ridges related to the oblique convergence of the margin (Nicol et al., 2007) Such tectonically-driven modification of bottom current pathways may well operate on longer time scales than those associated with the development of the studied drifts, which are all relatively young (i.e.,

of Late Miocene / Plio-Pleistocene to Recent age), but spatial variability in drift locations deeper in the stratigraphy might be anticipated, given that bottom currents have been documented off the east coast of the South Island since the Cretaceous (Fulthorpe et al., 2011).

Sediment waves located in the trench are characteristic of an area of the margin where changes in deformation style and lower slope gradients results in a less-tortuous bottom current pathways (Fig. 13). The outer slope of the subduction front and the Chatham Rise form broad trench boundaries to the sediment wave field of the Hikurangi Channel levee. It is suggested that these bathymetric boundaries deflect the abyssal deep-water currents, such as the north-bound DWBC and the south-bound Subtropical Front and ECC, forming complex gyrotory currents along the subduction front, which may erode the outer slope and interact with both channel and overbank deposits (*sensu* Carter and McCave, 2002; Migeon et al., 2006; Chiswell et al., 2015). More oceanographic data are required to better constrain bottom current pathways in this setting.





**Fig. 13** Conceptual diagram integrating the deposition of modern contourite drifts and their parental oceanographic bottom currents to illustrate the structural control on drift distribution along the convergent Hikurangi Margin. Note: abyssal bottom current pathways are poorly constrained.

### **Generic Implications for Drifts on Convergent Margins**

This study illustrates the importance of investigations to characterize the distribution of drifts along convergent margin settings; contourites in these settings may be more prevalent than was evident from earlier work. Although similar drift styles to those documented on other margin types are recognised, drifts along the Hikurangi Margin show significant differences in size, longevity, and morphology compared to drifts documented along passive margins (Table 3). In particular, most of the recognised drift types cover areas roughly one order of magnitude less than those of their passive margin counterparts. The size, thickness variations, and development of cross-cutting relationships described in this study can be attributed to the temporal and spatial evolution of the subduction wedge - related bathymetry, and its control upon the opening and closing of downslope current conduits and on the presence of along-slope currents that may modify gravity current deposits. Conversely, areas where gravity current deposits are apparent, but contourites are seemingly absent, could be a result of blocking or diversion of along-slope currents by growth structures, such as in the heavily deformed southern portion of the subduction wedge (Fig. 12; McArthur et al., 2019). These active margin controls result in drifts that are more restricted both spatially and temporally than drifts documented on passive margins, such as the Campos Margin (Faugères et al, 1998) and the Falklands Trough (Cunningham et al., 2002), where contourite accumulations evolving since the Cretaceous reach thicknesses of several kilometres.

There is a relative paucity of documented analogues for drifts located along convergent margins compared to the plethora of published drift examples from the north and south Atlantic and the Mediterranean Sea. Therefore, similar studies of other subduction complexes are recommended; margins at subtropical latitudes, i.e., in proximity to bottom waters derived from the poles, may be the best areas to focus such studies. Candidate regions for future investigation

include the Kerguelen Plateau (Fukamachi et al., 2010), the Southeast Indian Ridge (Joseph et al., 2002), and the Indonesian Archipelago (Dezileau et al., 2000).

**Table 3.** Summary of Drift Classification and Morphology

<b>Drift Types</b>	<b>Size</b>	<b>HM Drifts</b>	<b>Examples</b>
Giant elongated mounded drift	$10^3 - 10^5 \text{ km}^2$	$10 - 10^3 \text{ km}^2$	Erik drift, Greenland margin (Arthur et al., 1989); Blake-Bahama drifts, US margin (Mountain and Tucholke, 1985; McCave and Tucholke, 1986; Mulder et al., 2019).
Separated mounded drift	$10^3 - 10^4 \text{ km}^2$	$10 - 10^4 \text{ m}^2$	Feni drift, NE Rockall Trough (Kidd and Hill, 1986, 1987; Stoker, 1998; Howe et al., 1994); Faro drift, Gulf of Cadiz (Cremer et al., 1985; Mougnot, 1988).
Confined mounded drift	$10^3 - 10^5 \text{ km}^2$	$10 - 10^3 \text{ m}^2$	Sumba drift, S Indonesian margin (Reed et al., 1987); Louisville drift, E New Zealand (Carter and McCave, 1994)
Slope plastered sheet drift	$10^3 - 10^4 \text{ km}^2$	$<10 - 10^3 \text{ km}^2$	Gulf of Cadiz, Campos margin (Kenyon and Belderson, 1973; Faugeres et al., 1998); NE Chatham Rise, New Zealand (Wood and Davy, 1994).
Abyssal sheet drift	$10^5 - 10^6 \text{ km}^2$	$10^2 - 10^3 \text{ m}^2$	Gloria drift; Argentine Basin (Flood and Shor, 1988).
Mixed: Extended turbidite – contourite levee	$10^3 - 10^4 \text{ km}^2$	$10^2 - 10^3 \text{ m}^2$	Columbus levee, Brazil Basin (Faugeres et al., 1999, 2002); Hikurangi fan drift, New Zealand (Carter and Mitchell, 1987; Carter and Carter, 1988; Carter et al., 1990; Wood and Davy, 1994; McCave and Carter, 1997).
Mixed: Sculpted turbidite bodies	$10^3 - 10^4 \text{ km}^2$	$10 - 10^3 \text{ m}^2$	SE Weddell Sea (Weber et al., 1994; Cunningham, 1996).
Mixed: Intercalated turbidite – contourite bodies	Can be very extensive	$10 - 10^3 \text{ m}^2$	Hatteras Rise, E US margin (Mountain and Tucholke, 1985; McMaster et al., 1989; Locker and Laine, 1992); SE Brazilian margin (Souza Cruz, 1995; Faugeres et al., 1998).

## CONCLUSIONS

This study demonstrates the previously undocumented occurrence of contourite drifts along the Hikurangi subduction margin, New Zealand. Analysis of bathymetric and seismic datasets allows the recognition of mounded and sheeted drift types, contouritic moats and hybrid drifts comprising reworked gravity current deposits. A key control on the distribution of these drifts is likely the spatiotemporal evolution of the bathymetric ridges generated by subduction along this margin. Thus, the geometry of the subduction wedge influences the circulation of bottom currents along the margin, forming:

1. An upper slope drift trend around major intrabasinal structures. This trend is controlled by the uplift of the subduction wedge and the intermittent ability of contour currents to circulate along and around growing seafloor structures.
2. A spatiotemporally discontinuous trend of hybrid drifts within the trench-slope basins on the subduction wedge, where the historic and modern interaction of along-slope and downslope currents is recorded by intervals of gravity current sedimentation punctuated by bottom current reworking.
3. A hybrid drift trend within the relatively undeformed trench fill outboard of the subduction front. Here, the trench-axial Hikurangi Channel and its associated overbank sediment wave fields are crossed by abyssal bottom currents that appear locally to modify the channel form and overbank wave field.

Drift occurrence along this convergent margin is thought to vary with the orientation, strength and density properties of oceanographic bottom currents; drift style varies with the structurally controlled slope gradient and irregular seafloor topography. It is worth noting that the studied drifts are generally smaller, spatially less continuous, and temporally more punctuated in their development than drifts documented on passive margins. Further study is

recommended to assess how prevalent contourites are on other active margins, and whether the differences in drift type tie systematically to the tectonic configuration.

## ACKNOWLEDGEMENTS

We are grateful for the data access provided by the National Institute of Water and Atmosphere Research (NIWA), WesternGeco, and New Zealand Petroleum and Minerals (NZPM). Alex Karvelas and Tristan Allen (Schlumberger) are thanked for their help in arranging access to the WesternGeco Multiclient dataset, and Dan Tek for his help compiling oceanographic data. Associate editor Anna Pontén is thanked for handling our manuscript and reviewers Richard Wild and Arne Fuhrmann are thanked for their constructive comments.

## REFERENCES

- Argo** (2019) Argo float data and metadata from Global Data Assembly Centre (Argo GDAC). SEANOE. <http://doi.org/10.17882/42182>.
- Arthur, M.A., Srivastava, S.P., Kaminski, M., Jarrard, R. and Osler, J.** (1989) Seismic stratigraphy and history of deep circulation and sediment drift development in Baffin Bay and the Labrador Sea. *Proc. Ocean Drill. Program*, **105**(B), 891–922.
- Bailleul, J., Chanier, F., Ferrière, J., Robin, C., Nicol, A., Mahieux, G., Gorini, C. and Caron, V.** (2013) Neogene evolution of lower trench-slope basins and wedge development in the central Hikurangi subduction margin, New Zealand. *Tectonophysics*, **591**, 152–174.
- Barnes, P.M.** (1992) Mid-bathyal current scours and sediment drifts adjacent to the Hikurangi deep-sea turbidite channel, eastern New Zealand: evidence from echo character mapping. *Mar. Geol.*, **106**, 169–187.
- Barnes, P.M., Nicol, A. and Harrison, T.** (2002) Late Cenozoic evolution and earthquake potential of an active listric thrust complex above the Hikurangi subduction zone, New Zealand. *Geol. Soc. of Am. Bull.*, **114**, 1379-1405.
- Barnes, P.M., Lamarche, G., Bialas, J., Henrys, S., Pecher, I., Netzeband, G.L., Greinert, J., Mountjoy, J.J., Pedley, K. and Crutchley, G.** (2010) Tectonic and geological framework for gas hydrates and cold seeps on the Hikurangi subduction margin, New Zealand. *Mar. Geol.*, **272**(1-4), 26-48.
- Biros, D., Cuevas, R. and Moehl, B.** (1995) Well Completion Report Titihaoa-1, PPL 38318. In: New Zealand Open-file Petroleum Report 2018. Crown Minerals, Wellington. pp.1096.

- Bland, K.J., Uruski, C.I. and Isaac, M.J.** (2015) Pegasus Basin, eastern New Zealand: A stratigraphic record of subsidence and subduction, ancient and modern. *NZ J. Geol. Geophys.*, **58**(4), 319-343.
- Brackenridge, R.E., Hernández-Molina, F.J., Stow, D.A.V. and Llave, E.** (2013) A Pliocene mixed contourite–turbidite system offshore the Algarve Margin, Gulf of Cadiz: seismic response, margin evolution and reservoir implications. *Mar. Petrol. Geol.*, **46**, 36-50.
- Brodie, J. W.** (1960) Coastal surface currents around New Zealand. *NZ J. Geol. Geophys.*, **3**(2), 235-252.
- Carter, L., and Mitchell, J.S.** (1987) Late Quaternary sediment pathways through the deep ocean, east of New Zealand. *Paleoceanography*, **2-4**, 409–422.
- Carter, L., Carter, R.M., Nelson, C.S., Fulthorpe, C.S. and Neil, H.L.** (1990) Evolution of Pliocene to recent abyssal sediment waves on Bounty channel levees, New Zealand. *Mar. Geol.*, **95**, 97–109.
- Carter, L. and McCave, I.N.** (1994) Development of sediment drifts approaching an active plate margin under the SW Pacific Deep Western Boundary Current. *Paleoceanography*, **9**(6), 1061-1085.
- Carter, L. and McCave, I.N.** (2002) Eastern New Zealand Drifts, Miocene-Recent. *Geol. Soc. London, Mem.*, **22**(1), 385-407.
- Carter, L., Carter, R.M., McCave, I.N. and Gamble, J.** (1996) Regional sediment recycling in the abyssal Southwest Pacific Ocean. *Geology*, **24**(8), 735-738.
- Carter, L., Carter, R.M. and McCave, I.N.** (2004) Evolution of the sedimentary system beneath the deep Pacific inflow off eastern New Zealand. *Mar. Geol.*, **205**(1-4), 9-27.
- Chanier, F., Ferriere, J. and Angelier, J.** (1999) Extensional deformation across an active margin, relations with subsidence, uplift, and rotation: the Hikurangi subduction, New Zealand. *Tectonics*, **18**, 862-876.
- Chen, H., Xie, X., Van Rooij, D., Vandorpe, T., Su, M. and Wang, D.** (2014) Depositional characteristics and processes of alongslope currents related to a seamount on the northwestern margin of the Northwest Sub-Basin, South China Sea. *Mar. Geol.*, **355**, 36–53.
- Chen, H., Zhang, W., Xie, X. and Ren, J.** (2019) Sediment dynamics driven by contour currents and mesoscale eddies along continental slope: A case study of the northern South China Sea. *Mar. Geol.*, **409**, 48-66.
- Chiswell, S.M. and Roemmich, D.** (1998) The East Cape Current and two eddies: A mechanism for larval retention? *NZ J. Mar. Freshwat. Res.*, **32**(3), 385-397.
- Chiswell, S.M., Bostock, H.C., Sutton, P.J. and Williams, M.J.** (2015) Physical oceanography of the deep seas around New Zealand: a review. *NZ J. Mar. Freshwat. Res.*, **49**(2), 286-317.
- Cremer, M., Orsolini, P. and Ravenne, C.** (1985) Cap Ferret Fan, Atlantic Ocean. In: Bouma, A.H., Normak, W.R., Barnes, N.E. Eds., *Submarine Fans and Related Turbidite Systems*. Springer-Verlag, New York. pp. 113–120.
- Crutchley, G.J., Mountjoy, J.J., Kellet, R.L., Black, J., Bland, K.J., Coffin, R.B., Field, B., Henrys, S.A., Neil, H.L., O'Brien, G., Pecher, I.A., Rose, P.S., Stagpoole, V.M. and**

- Strogen, D.P.** (2016) Petroleum prospectivity screening report of the offshore northern East Coast Basin, *GNS Science Consultancy Report 2015/225*. pp.155.
- Cunningham, A.P., Howe, J.A. and Barker, P.F.** (2002) Contourite sedimentation in the Falkland Trough, western South Atlantic. *Geol. Soc. London, Mem.*, 22(1), 337-352.
- Davy, B., Hoernle, K. and Werner, R.** (2008) Hikurangi Plateau: Crustal structure, rifted formation, and Gondwana subduction history. *Geochemistry, Geophysics, Geosystems*, 9(7).
- Dezileau, L., Bareille, G., Reyss, J.L. and Lemoine, F.** (2000) Evidence for strong sediment redistribution by bottom currents along the southeast Indian ridge. *Deep-Sea Res. Part I: Oceanograph. Res. P.*, 47(10), 1899-1936.
- Dorrell, R. M., Peakall, J., Darby, S. E., Parsons, D. R., Johnson, J., Sumner, E. J., Wynn, R. B., Ozsoy, E. and Tezcan, D.** (2019) Self-sharpening induces jet-like structure in seafloor gravity currents. *Nature Communications* (10)10.
- Ercilla, G., Juan, C., Hernández-Molina, F.J., Bruno, M., Estrada, F., Alonso, B., Casas, D., Farran, M. I., Llave, E., García, M., Vázquez, J.T., D'Acromont, E., Gorini, C., Palomino, D., Valencia, J., El Mounni, B. and Ammar, A.** (2016) Significance of bottom currents in deep-sea morphodynamics: An example from the Alboran Sea. *Mar. Geol.*, 378, 157–170.
- Faugères, J.C. and Gonthier, E.** (1997) Deep marine deposits controlled by contour currents: the case of the Gulf of Cadiz. 2<sup>nd</sup> Symposium on the Atlantic Iberian margin, Cadiz, Abstract Volume. University of Cadiz. pp. 131–132.
- Faugères, J.C. and Stow, D.A.V.** (1993) Bottom-current-controlled sedimentation: a synthesis of the contourite problem. *Sediment. Geol.*, 82, 287–297.
- Faugères, J.C., Me´zerai, M.L. and Stow, D.A.V.** (1993b) Contourite drift types and their distribution in the North and South Atlantic Ocean basins. *Sediment. Geol.*, 82(1–4), 189–203.
- Faugères, J.C., Imbert, P., Mezerai, M.L. and Cremer, M.** (1998) Seismic patterns of a muddy contourite fan (Vema Channel, South Brazilian Basin and a sandy deep-sea fan) Cap Ferret system Bay of Biscay: a comparison. *Sediment. Geol.*, 115(1–4), 81–110.
- Faugères, J.C., Lima, A.F., Massé, L. and Zaragosi, S.** (2002) The Columbia channel-levee system: a fan drift in the southern Brazil Basin. *Geol. Soc. London, Mem.*, 22(1), 223-238.
- Faugères, J.C. and Mulder, T.** (2011) Contour currents and contourite drifts. *Dev. Sedimentol.*, 63, 149-214.
- Faugères, J.C., Stow, D.A., Imbert, P. and Viana, A.** (1999) Seismic features diagnostic of contourite drifts. *Mar. Geol.*, 162(1), 1-38.
- Flood, R.D.** (1994) Abyssal bedforms as indicators of changing bottom current flow: examples from the US East Coast continental rise. *Paleoceanography*, 9(6), 1049-1060.
- Flood, R.D. and Shor, A.N.** (1988) Mudwaves in the Argentine Basin and their relationship to regional bottom circulation patterns. *Deep-Sea Res.* 35, 943–972.
- Fonnesu, M., Palermo, D., Galbiati, M., Marchesini, M., Bonamini, E. and Bendias, D.** (2020) A new world-class deep-water play-type, deposited by the syndepositional interaction



of turbidity flows and bottom currents: The giant Eocene Coral Field in northern Mozambique. *Mar. Petrol. Geol.*, **111**, 179-201.

**Fuhrmann, A., Kane, I.A., Clare, M.A., Ferguson, R.A., Schomacker, E., Bonamini, E. and Contreras, F.A.** (2020) Hybrid turbidite-drift channel complexes: An integrated multiscale model. *Geology*.

**Fukamachi, Y., Rintoul, S.R., Church, J.A., Aoki, S., Sokolov, S., Rosenberg, M.A. and Wakatsuchi, M.** (2010) Strong export of Antarctic Bottom Water east of the Kerguelen plateau. *Nature Geoscience*, **3**(5), 327.

**Fulthorpe, C.S. and Carter, R.M.** (1991) Continental shelf progradation by sediment drift accretion. *Geol. Soc. Am. Bull.*, **103**(2), 300–309.

**Fulthorpe, C.S., Hoyanagi, K., Crundwell, M.P., Dinarès-Turell, J., Ding, X., George, S.C., Hepp, D.A., Jaeger, J., Kawagata, S., Kemp, D.B. and Kim, Y.G.** (2011) Expedition 317 summary. In Proceedings of the Integrated Ocean Drilling Program. Integrated Ocean Drilling Program Management International, **317**, 1-86.

**Gong, C., Wang, Y., Zhu, W., Li, W. and Xu, Q.** (2013) Upper Miocene to Quaternary unidirectionally migrating deep-water channels in the Pearl River mouth Basin, northern South China Sea. *AAPG Bull.*, **97**(2), 285-308.

**Heath, R.A.** (1985) A review of the physical oceanography of the seas around New Zealand—1982. *NZ J. Mar. Freshwat. Res.*, **19**(1), 79-124.

**Heezen, B.C. and Hollister, C.** (1964) Deep-sea current evidence from abyssal sediments. *Mar. Geol.*, **1**(2), 141-174.

**Heezen, B.C. and Hollister, C.D.** (1971) *Face of the deep*. Oxford University. pp.659.

**Heezen, B.C., Hollister, C.D. and Ruddiman, W.F.** (1966) Shaping of the continental rise by deep geostrophic bottom currents. *Sciences*, **152**, 502–508.

**Hernández-Molina, F.J., Larter, R.D., Rebesco, M. and Maldonado, A.** (2006) Miocene reversal of bottom water flow along the Pacific Margin of the Antarctic Peninsula: stratigraphic evidence from a contourite sedimentary tail. *Mar. Geol.*, **228**, 93–116.

**Hernández-Molina, F.J., Maldonado, A. and Stow, D.A.V.** (2008a) Abyssal plain contourites. In: Rebesco, M., Camerlenghi, A. (Eds.), *Contourites. Dev. Sedimentol.*, **60**, Amsterdam, 345–378.

**Hernández-Molina, F.J., Stow, D.A.V. and Llave** (2008b) Continental slope contourites. In: Rebesco, M., Camerlenghi, A. (Eds.), *Contourites. Dev. Sedimentol.*, **60**, Amsterdam, 379–408.

**Hernández-Molina, F.J., Llave, E., Preu, B., Ercilla, G., Fontan, A., Bruno, M., Serra, N., Gomiz, J.J., Brackenridge, R.E., Sierro, F.J. and Stow, D.A.** (2014) Contourite processes associated with the Mediterranean Outflow Water after its exit from the Strait of Gibraltar: Global and conceptual implications. *Geology*, **42**(3), 227-230.

**Hollister, C.D. and Heezen, B.C.** (1972) Geological effects of ocean bottom currents: western North Atlantic. In: Gordon, A.L. (Ed.), *Studies in Physical Oceanography*, **2**. Gordon and Breach, New York, 37–66.

**Hollister, C.D. and McCave, N.** (1984) Sedimentation under benthic storms. *Nature*, **309**, 220–225.

- Hollister, C.D., Johnson, D.A. and Lonsdale, P.** (1974) Current-control abyssal sedimentation: Samoan Passage, equatorial west Pacific. *J. Geol.*, **82**, 275–300.
- Howe, J., Stoker, M.S. and Stow, D.A.V.** (1994) Late Cenozoic sediment drift complex, Northeast Rockall Trough. *Paleoceanography* **9**(6), 989–999.
- Ivchenko, V.O., Richards, K.J. and Stevens, D.P.** (1996) The dynamics of the Antarctic circumpolar current. *J. Phys. Oceanograph.*, **26**(5), 753–774.
- Johnson, D.A. and Peters, C.S.** (1979) Late Cenozoic sedimentation and erosion on the Rio Grande Rise. *J. Geol.*, **87**(4), 371–392.
- Joseph, L.H., Rea, D.K., van der Pluijm, B.A. and Gleason, J.D.** (2002) Antarctic environmental variability since the late Miocene: ODP Site 745, the East Kerguelen sediment drift. *Earth Planet. Sci. Lett.*, **201**(1), 127–142.
- Juan, C., Van Rooij, D. and De Bruycker, W.** (2018) An assessment of bottom current controlled sedimentation in Pacific Ocean abyssal environments. *Mar. Geol.*, **403**, 20–33.
- Kneller, B., Dykstra, M., Fairweather, L. and Milana, J.P.** (2016) Mass-transport and slope accommodation: implications for turbidite sandstone reservoirs. *AAPG Bull.*, **100**(2), 213–235.
- Kidd, R.B. and Hill, P.R.** (1987) Sedimentation on Feni and Gardar sediment drifts. Initial Rep. Deep Sea Drill Project. US Govt. Printing Office, Washington, **94**, 1217–1244.
- Knutz, P.C.** (2008) Palaeoceanographic significance of contourite drifts. *Dev. Sedimentol.*, **60**, 511–535.
- Laberg, J.S., Baeten, N.J., Vanneste, M., Forsberg, C.F., Forwick, M. and Haflidason, H.** (2016) Sediment failure affecting muddy contourites on the continental slope offshore northern Norway: lessons learned and some outstanding issues. In *Submarine Mass Movements and their Consequences* (pp. 281–289). Springer, Cham.
- Ledbetter, M.T.** (1984) Bottom-current speed in the Vema Channel recorded by particle size of sediment fine-fraction. *Mar. Geol.*, **58**, 137–149.
- Ledbetter, M.T.** (1986) Bottom-current pathways in the Argentine Basin revealed by mean silt particle size. *Nature*, **321**(6068), 423–425.
- Lewis, K.B. and Pantin, H.M.** (2002) Channel-axis, overbank and drift sediment waves in the southern Hikurangi Trough, New Zealand. *Mar. Geol.*, **192**(1–3), 123–151.
- Lewis, K.B. and Pettinga, J.R.** (1993) The emerging, imbricate frontal wedge of the Hikurangi margin. *Sedimentary basins of the world*, **2**, 225–250.
- Locker, S.D. and Laine, P.** (1992) Paleogene–Neogene depositional history of the middle, US Atlantic continental rise: mixed turbidite and contourite depositional systems. *Mar. Geol.*, **103**, 137–164.
- Lonsdale, P.** (1981) Drifts and ponds of reworked pelagic sediment in part of the Southwest Pacific. *Mar. Geol.*, **43**, 153–193.
- Masse, L., Faugères, J.C., Bernat, M., Pujos, A. and Mezerai, M.L.** (1994) A 600,000-year record of Antarctic Bottom Water activity inferred from sediment textures and structures in a sediment core from the Southern Brazil Basin. *Paleoceanography* **9**(6), 1017–1026.

- Masse, L., Faugères, J.C. and Hrovatin, D.** (1998) The interplay between turbidity and contour current processes on the Columbia Channel fan drift, Southern Brazilian Basin. *Sediment. Geol.*, **115**, 111–132.
- McArthur, A.D. and McCaffrey, W.D.** (2019) Sedimentary architecture of detached deep-marine canyons: Examples from the East Coast Basin of New Zealand. *Sedimentology*, **66**, 1067–1101.
- McArthur, A.D., Claussmann, B., Bailleul, J., McCaffrey, W. and Clare, A.** (2019) Variation in syn-subduction sedimentation patterns from inner to outer portions of deep-water fold and thrust belts: examples from the Hikurangi subduction margin of New Zealand. *Geol. Soc. London, Spec. Publ.*, **490**, 490–545.
- McCave, I.N. and Tucholke, B.E.** (1986) Deep current-controlled sedimentation in the western North Atlantic. *The Geology of North America*, **1000**, 451–468.
- McCave, I.N. and Carter, L.** (1997) Recent sedimentation beneath the Deep Western Boundary Current off northern New Zealand. *Deep-Sea Res., Part I* **44**(7), 1203–1237.
- McCave, I.N., Manighetti, B. and Beveridge, N.A.S.** (1995) Circulation in the glacial North Atlantic inferred from grain-size measurements. *Nature*, **374**, 149–152.
- McMaster, R.L., Locker, S.D. and Laine, E.P.** (1989) The early Neogene continental rise off the eastern United States. *Mar. Geol.*, **87**, 123–137.
- Migeon, S., Mulder, T., Savoye, B. and Sage, F.** (2006) The Var turbidite system (Ligurian Sea, northwestern Mediterranean)—morphology, sediment supply, construction of turbidite levee and sediment waves: implications for hydrocarbon reservoirs. *Geo- Marine Lett.*, **26**, 361–371.
- Miramontes, E., Garziglia, S., Sultan, N., Jouet, G. and Cattaneo, A.** (2018) Morphological control of slope instability in contourites: a geotechnical approach. *Landslides*, **15**(6), 1085–1095.
- Mougenot, D.** (1988) *Geologie de la marge portugaise*. These de Doctorat d’Etat, Universite Paris VI, p. 257.
- Mountain, G.S. and Tucholke, B.E.** (1985) Mesozoic and Cenozoic geology of the US Atlantic continental slope and rise. In: Poag, C.W. (Ed.), *Geologic Evolution of the United States Atlantic Margin*, pp. 293–341.
- Mountjoy, J.J., Barnes, P.M. and Pettinga, J.R.** (2009) Morphostructure and evolution of submarine canyons across an active margin: Cook Strait sector of the Hikurangi Margin, New Zealand. *Mar. Geol.*, **260**(1–4), 45–68.
- Mountjoy, J.J., Micallef, A., Stevens, C.L. and Stirling, M.W.** (2014) Holocene sedimentary activity in a non-terrestrially coupled submarine canyon: Cook Strait Canyon system, New Zealand. *Deep-Sea Res. Part II: Top. Stud. Oceanograph.*, **104**, 120–133.
- Mountjoy, J.J., Howarth, J.D., Orpin, A.R., Barnes, P.M., Bowden, D.A., Rowden, A.A., Schimel, A.C., Holden, C., Horgan, H.J., Nodder, S.D. and Patton, J.R.** (2018) Earthquakes drive large-scale submarine canyon development and sediment supply to deep-ocean basins. *Sci. Adv.*, **4**(3), 3748.

**Mulder, T., Lecroart, T.P., Voisset, M., Schönfeld, J., Le Drezen, E., Gonthier, E., Hanquiez, V., Zahn, R., Faugères, J.C., Hernández-Molina, F.J. and Llave-Barranco, E.** (2002) Past deep - ocean circulation and the paleoclimate record - Gulf of Cadiz. *EOS, Transactions American Geophysical Union*, **83**(43), 481-488.

**Mulder, T., Faugères, J.C. and Gonthier, E.** (2008) Mixed turbidite–contourite systems. *Dev. Sedimentol.*, **60**, 435-456.

**Mulder, T., Ducassou, E., Hanquiez, V., Principaud, M., Fauquembergue, K., Tournadour, E., Chabaud, L., Reijmer, J., Recouvreur, A., Gillet, H. and Borgomano, J.** (2019) Contour current imprints and contourite drifts in the Bahamian archipelago. *Sedimentology*, **66**(4), 1192-1221.

**Nicol, A., Mazengarb, C., Chanier, F., Rait, G., Uruski, C. and Wallace, L.** (2007) Tectonic evolution of the active Hikurangi subduction margin, New Zealand, since the Oligocene. *Tectonics*, **26**(4), pp.

**Normark, W. R., Piper, D. J. W., Posamentier, H., Pirmez, C. and Migeon, S.** (2002). Variability in form and growth of sediment waves on turbidite channel levees. *Mar. Geol.*, **192**(1-3), 23-58.

**Palermo, D., Galbiati, M., Famiglietti, M., Marchesini, M., Mezzapesa, D. and Fonnesu, F.** (2014) Insights into a new super-giant gas field-sedimentology and reservoir modelling of the Coral Reservoir Complex, Offshore Northern Mozambique. In *Offshore Technology Conference-Asia*. Offshore Technology Conference.

**Paquet, F., Proust, J.N., Barnes, P.M. and Pettinga, J.R.** (2009) Inner-forearc sequence architecture in response to climatic and tectonic forcing since 150 ka: Hawke's Bay, New Zealand. *J. Sed. Res.*, **79**(3), 97-124.

**Posamentier, H.W. and Kolla, V.** (2003) Seismic geomorphology and stratigraphy of depositional elements in deep-water settings. *J. Sed. Res.*, **73**(3), 367-388.

**Prather, B.E.** (2003) Controls on reservoir distribution, architecture and stratigraphic trapping in slope settings. *Mar. Petrol. Geol.*, **20**(6-8), 529-545.

**Preu, B., Hernández-Molina, F.J., Violante, R., Piola, A.R., Paterlini, C.M., Schwenk, T., Voigt, I., Krastel, S. and Spiess, V.** (2013) Morphosedimentary and hydrographic features of the northern Argentine margin: the interplay between erosive, depositional and gravitational processes and its conceptual implications. *Deep-Sea Res. Part I: Oceanogr. Res. Papers*, **75**, 157-174.

**Pudsey, C.J. and Howe, J.A.** (1998) Quaternary history of the Antarctic Circumpolar Current: evidence from the Scotia Sea. *Mar. Geol.*, **148**, 83–112.

**Rebesco, M. and Stow, D.** (2001) Seismic expression of contourites and related deposits: a preface. *Mar. Geophys. Res.*, **22**(5-6), 303-308.

**Rebesco, M., Larter, R.D., Camerlenghi, A. and Barker, P.F.** (1996) Giant sediment drifts on the continental rise west of the Antarctic Peninsula. *Geo-Mar. Lett.*, **16**, 65–75.

**Rebesco, M., Wählin, A., Laberg, J.S., Schauer, U., Beszczynska-Möller, A., Lucchi, R.G., Noormets, R., Accettella, D., Zarayskaya, Y. and Diviaco, P.** (2013) Quaternary contourite drifts of the Western Spitsbergen margin. *Deep-Sea Res. Part I: Oceanogr. Res. Papers*, **79**, 156-168.

- Rebesco, M., Hernández-Molina, F.J., Van Rooij, D. and Wåhlin, A.** (2014) Contourites and associated sediments controlled by deep-water circulation processes: state-of-the-art and future considerations. *Mar. Geol.*, **352**, 111-154.
- Reed, D.L., Meyer, A.W., Silver, E.A. and Prasetyo, H.** (1987) Contourite sedimentation in an intraoceanic forearc system: eastern Sunda Arc, Indonesia. *Mar. Geol.*, **76**, 223-241.
- Saffer, D.M., Wallace, L.M., Petronotis, K., Barnes, P.B., Bell, R.B., Crundwell, M.C., De Oliveira, C.H.E., Fagereng, A., Fulton, P.F., Greve, A. and Harris, R.H.** (2018) International ocean discovery program expedition 375 preliminary report: Hikurangi subduction margin coring and observatories unlocking the secrets of slow slip through drilling to sample and monitor the forearc and subducting plate, 8 March-5 May 2018. pp. 1-38.
- Sansom, P.** (2018) Hybrid turbidite–contourite systems of the Tanzanian margin. *Petrol. Geosci.*, **24**(3), 258-276.
- Schut, E.W. and Uenzelmann-Neben, G.** (2005) Cenozoic bottom current sedimentation in the Cape Basin, South Atlantic. *Geophys. J. International*, **161**(2), 325-333.
- Shanmugam, G., Spalding, T.D. and Rofheart, D.H.** (1993) Process Sedimentology and Reservoir Quality of Deep-Marine Bottom-Current Reworked Sands (Sandy Contourites): An Example from the Gulf of Mexico. *Am. Assoc. Pet. Geol. Bull.*, **77**, 1241–1259.
- Smillie, Z., Stow, D. and Esentia, I.P.** (2018) Deep-sea contourites drifts, erosional features and bedforms. *Encyclopedia of Ocean Sciences: Earth Systems and Environmental Sciences*. Elsevier. pp.
- Souza Cruz, C.E.** (1995) Estratigrafia e sedimentação de águas profundas do Neogeno da bacia de Campos, Estado do Rio de Janeiro, Brazil. PhD Thesis. UFRGS, Porto Alegre.
- Stevens, C.L., O’Callaghan, J.M., Chiswell, S.M. and Hadfield, M.G.** (2019) Physical oceanography of New Zealand/Aotearoa shelf seas, a review. *NZ J. Mar. Freshwat. Res.*, 1-40.
- Stickley, C.E., Carter, L., McCave, I.N. and Weaver, P.P.E.** (2001) Lower Circumpolar Deep Water flow through the SW Pacific Gateway for the last 190 ky: evidence from Antarctic diatoms. In Seidov, D., Haupt, B.J., and Maslin, M. (Eds.), *The Oceans and Rapid Climate Change. Geophys. Monogr.*, **126**, 101–116.
- Stramma, L., Peterson, R.G. and Tomczak, M.** (1995) The South Pacific Current. *J. Phys. Oceanogr.*, **25**, 77–91.
- Stoker, M.S., Akhurst, C., Howe, J.A. and Stow, D.A.V.** (1998) Sediment drifts and contourites on the continental margin, off Northwest Britain. *Sediment. Geol.*, **115**(1–4), 33–52.
- Stow, D.A.V. and Lovell, J.P.B.** (1979) Contourites: their recognition in modern and ancient sediments. *Earth-Sci. Rev.*, **14**(3), 251-291.
- Stow, D.A.V., Reading, H.G. and Collinson, J.** (1996) Deep Seas. In: Reading, H.G. (Ed.), *Sedimentary Environments*, 3rd ed., pp. 395–453.

- Stow, D.A., Faugères, J.C., Howe, J.A., Pudsey, C.J. and Viana, A.R.** (2002) Bottom currents, contourites and deep-sea sediment drifts: current state-of-the-art. *Geol. Soc., London, Mem.*, **22**(1), 7-20.
- Stow, D.A.V., Hunter, S., Wilkinson, D. and Hernández-Molina, F.J.** (2008) The nature of contourite deposition. *Dev. Sedimentol.*, **60**, 143-156.
- Stow, D., Smillie, Z., Pan, J. and Esentia, I.P.** (2018) Deep-Sea Contourites: Sediments and Cycles. *Encyclopedia of Ocean Sciences: Earth Systems and Environmental Sciences*. Elsevier. **4**, 111-120.
- Tap Oil Limited.** (2004) Tawatawa-1 Well Completion Report: PR3067. Crown Minerals. Wellington, New Zealand. pp. 873.
- Thran, A.C., Dutkiewicz, A., Spence, P. and Müller, R.D.** (2018) Controls on the global distribution of contourite drifts: Insights from an eddy-resolving ocean model. *Earth Planet. Sci. Lett.*, **489**, 228-240.
- Toucanne, S., Mulder, T., Schönfeld, J., Hanquiez, V., Gonthier, E., Duprat, J., Cremer, M. and Zaragosi, S.** (2007) Contourites of the Gulf of Cadiz: a high-resolution record of the paleocirculation of the Mediterranean outflow water during the last 50,000 years. *Palaeogeography, Palaeoclimatology, Palaeoecology*, **246**(2-4), 354-366.
- Trewick, S.A. and Bland, K.J.** (2012) Fire and slice: palaeogeography for biogeography at New Zealand's North Island/South Island juncture. *J. Royal Soc. New Zealand*, **42**(3), 153-183.
- Van Rooij, D., Iglesias, J., Hernández-Molina, F.J., Ercilla, G., Gomez-Ballesteros, M., Casas, D., Llave, E., De Hauwere, A., García-Gil, S., Acosta, J. and Henriot, J.P.** (2010) The Le Danois Contourite Depositional System: interactions between the Mediterranean outflow water and the upper Cantabrian slope (North Iberian margin). *Mar. Geol.*, **274**(1-4), 1-20.
- Viana, A.R., Almeida, W., Nunes, M.C.V. and Bulhões, E.M.** (2007) The economic importance of contourites. *Geol. Soc., London, Spec. Publ.*, **276**, 1-23.
- Viana, A. R.** (2008) Economic relevance of contourites. In: Rebesco, M. and Camerlenghi, A. (Eds). *Contourites. Dev. Sedimentol.*, **60**, 493-510.
- Vinnels, J.S., Butler, R.W.H., McCaffrey, W.D. and Paton, D.A.** (2010) Depositional processes across the Sinu accretionary prism, offshore Colombia. *Mar. Petrol. Geol.*, **27**, 794–809.
- Wallace, L.M., Barnes, P., Beavan, J., Dissen, R. Van, Litchfield, N., Mountjoy, J., Langridge, R., Lamarche, G. and Pondard, N.** (2012) The kinematics of a transition from subduction to strike-slip : An example from the central New Zealand plate boundary. *J. Geophys. Res.*, **117**, 1–24.
- Warren, B.A.** (1981) Deep circulation in the world ocean. In Warren, B.A., and Wunsch, C. (Eds.), *Evolution of Physical Oceanography*: Cambridge (MIT Press), pp. 6–42.
- Weber, M.E., Bonani, G. and Futterer, K.D.** (1994) Sedimentation processes within channel–ridge systems, southeastern Weddell Sea, Antarctica. *Paleoceanography* **9**(6), 1027–1048.
- Wong, H.K., Lüdmann, T., Baranov, B.V., Karp, B.Y., Konerding, P. and Ion, G.** (2003) Bottom current-controlled sedimentation and mass wasting in the northwestern Sea of Okhotsk. *Mar. Geol.*, **201**(4), 287-305.

**Wood, R. and Davy, B.** (1994) The Hikurangi Plateau. *Mar. Geol.*, **118**(1-2), 153-173.

**Wynn, R. B. and Masson, D. G.** (2008) Sediment Waves and Bedforms. In: Rebesco, M. and Camerlenghi, A. (Eds). *Contourites. Developments in Sedimentology*, Amsterdam, Elsevier Science Bv 60: 289-300.

**Wynn, R.B. and Stow, D.A.** (2002) Classification and characterisation of deep-water sediment waves. *Mar. Geol.*, **192**(1-3), 7-22.